AMERICAN JOURNAL OF PHYSIOLOGY
CELL PHYSIOLOGY

Am J Physiol Cell Physiol 329: C1825–C1841, 2025.
First published October 6, 2025; doi:10.1152/ajpcell.00533.2025

RESEARCH ARTICLE

Skeletal muscle alterations and functional repercussions in patients with colorectal cancer-associated cachexia

Britt van de Haterd,[1] Michèlle Hendriks,[1] Bert Houben,[2] Michelle E. G. Weijzen,[1] Frank Vandenabeele,[3] Kenneth Verboven,[1,4] and Anouk Agten[5,6]

[1]*REVAL-Rehabilitation Research Centre, Hasselt University, Diepenbeek, Belgium;* [2]*Department of Abdominal Surgery, Jessa Hospital, Hasselt, Belgium;* [3]*Dokterspraktijk Vandenabeele-Craenen, Alken, Belgium;* [4]*BIOMED-Biomedical Research Institute, Hasselt University, Diepenbeek, Belgium;* [5]*U-RISE-UHasselt Research Group on Innovative and Society-Engaged Education, School for Educational Studies, Hasselt University, Diepenbeek, Belgium; and* [6]*Faculty of Medicine and Life Sciences, department of anatomy, Hasselt University, Diepenbeek, Belgium*

Abstract

Cancer cachexia causes skeletal muscle wasting and metabolic dysfunction, worsening clinical outcomes in colorectal cancer (CRC). This study examines microscopic and macroscopic skeletal muscle fiber characteristics, and muscle volume in patients with CRC-associated cachexia and without cachexia compared with healthy controls (HCs), and explores how these factors relate to physical performance. In total, 12 patients with CRC-associated cachexia, 25 CRC patients without cachexia, and 25 HCs were included. Cachexia was determined by weight loss and Cachexia Staging Score. Biopsies from the vastus lateralis and erector spinae muscles were analyzed using immunohistochemistry for muscle fiber type cross-sectional area (CSA) and distribution, myonuclear content, and capillary density. Muscle volume was assessed using three-dimensional ultrasound, and CSA and density by computerized tomography scans. Physical function was evaluated with the Short Physical Performance Battery test, handgrip strength, and the Physical Activity Scale for Individuals with Physical Disabilities. Quality of life was assessed using the 36-item Short Form Survey. Patients with CRC-associated cachexia showed reduced type II muscle fiber CSA in the vastus lateralis compared with HCs and CRC patients without cachexia. CRC Patients without cachexia exhibited a slow-to-fast muscle fiber shift compared with HCs. Myonuclear content was lower in both cancer groups. Muscle volume and density were reduced in patients with CRC-associated cachexia. Positive correlations were found between microscopic and macroscopic skeletal muscle characteristics, muscle strength, physical performance, and quality of life, respectively. CRC Patients, especially those with cachexia, showed type II muscle fiber atrophy, reduced myonuclear content, and impaired physical function, emphasizing the need for targeted prehabilitation interventions.

NEW & NOTEWORTHY This study reveals skeletal muscle alterations in colorectal cancer patients with cachexia, at microscopic (fiber-type specific atrophy, myonuclear content, and capillarization) and macroscopic levels (muscle volume and quality). These alterations were associated with clinically important measures of physical functioning and quality of life. Collectively, these findings establish clinically relevant links between structural muscle alterations and physical outcomes, highlighting the potential value of targeted (p)rehabilitation interventions in these patient populations.

cachexia; colorectal cancer; cross-sectional area; muscle atrophy; muscle fiber typing

INTRODUCTION

Cancer cachexia (CC) is a multifactorial syndrome characterized by severe, unintentional weight loss, comprising both adipose tissue and muscle mass loss, significantly impacting patients' quality of life, response to therapy, and prognosis (1–5). In CC, a persistent negative protein and energy balance, which is driven by tumor-derived factors and systemic inflammatory responses, promotes muscle wasting and adipose tissue depletion (6–9). The prevalence of cachexia varies across cancer types, affecting up to 60% of patients with colorectal cancer (CRC), especially in advanced stages (10). Factors such as tumor location, stage, and presence of metastasis influence cachexia severity, highlighting the complexity of this syndrome across patients (11, 12).

Skeletal muscle is a highly dynamic tissue and comprises various muscle fiber types with distinct metabolic and functional properties. Type I (slow-twitch) fibers, rich in mitochondria and capillaries, support endurance activities, whereas type II (fast-twitch) fibers, including type IIa and IIx, provide power but are more quickly susceptible to fatigue (13–15). Most preclinical (16–19) and human studies (20, 21) on CC indicate atrophy in both fiber types, whereas other preclinical (22–24) and human studies (25, 26) suggest that type II muscle fibers are more affected. Although one study reports a shift toward type II fibers in patients with pancreatic cachexia and CRC

Correspondence: B. van de Haterd (britt.vandehaterd@uhasselt.be).
Submitted 2 July 2025 / Revised 22 July 2025 / Accepted 15 September 2025

cachexia (27), others find no changes in fiber distribution (20, 21, 28). Myonuclei, critical for muscle maintenance and adaptation, may be lost more slowly than muscle fiber size (29). In CC, myonuclei display typically more in the center of muscle fibers, which is associated with muscle wasting (30). Capillary density influences muscle metabolism and may affect susceptibility to atrophy, with CC-related muscle loss linked to hypoxia-induced capillary regression, being further exacerbated by systemic inflammation (31–34).

Research on CC mechanisms and changes in skeletal muscle characteristics has primarily been performed in preclinical models (e.g., C26 colon carcinoma mouse model, Lewis lung carcinoma mouse model, adenomatous polyposis coli (APC)Min/+ mouse model) (35). Human studies on CC, and more specific CRC-related cachexia, are limited, as former studies on CC often focus on lung (20, 25), gastrointestinal (21, 26, 27), and pancreatic cancer (26–28). Of particular importance to human patients, muscle fiber atrophy in CC leads to decreased muscle mass and function, reducing physical performance and daily activity levels (30, 36, 37). In contrast, computed tomography (CT) of the *m. erector spinae* has been described to be attenuated in human patients with CC (8, 38–41).

This cross-sectional study aims to evaluate both microscopic [e.g., skeletal muscle fiber cross-sectional area (CSA) and distribution, myonuclear content, and capillary density] and macroscopic (e.g., skeletal muscle volume and quality) skeletal muscle characteristics in patients with CRC-associated cachexia and without cachexia compared with healthy controls (HCs). In addition, the study explores interrelationships between skeletal muscle characteristics and clinical indicators of physical function. By elucidating the structural and functional muscle alterations in CRC-associated cachexia, this research seeks to inform targeted interventions to mitigate muscle wasting in patients with CRC, ultimately improving patient treatment outcomes and quality of life.

MATERIALS AND METHODS

Subjects and Study Design

This cross-sectional study included 12 patients with CRC-associated cachexia, 25 CRC patients without cachexia, and 25 HCs. Recruitment of the CRC patients was done at the Department of Abdominal Surgery (Jessa Hospital, Hasselt, Belgium) and HCs via professional social media platforms of the Hasselt University. The group with the CRC patients without cachexia and the HCs were matched for sex and age, no matching was performed for the patients with CRC-associated cachexia.

Patients with CRC-associated cachexia met the following criteria: *1*) age $\geq$ 18 yr, *2*) unintentional weight loss >5% over last 6 mo or >2% with Body Mass Index (BMI) <20 kg/m^2 or sarcopenia based on the diagnostic criterion stated by Fearon et al. (11), and *3*) cachexia staging score (CSS) between 5 and 12. The cachexia staging score (CSS), developed by Zhou at al. (42), provides a tool for classifying the stages of cachexia in patients with cancer. The score is based on the assessment of five domains: weight loss, risk of sarcopenia, functional status and overall health, appetite loss, and abnormal blood biochemistry. A total score between 0 and 2 corresponds to noncachexia, a score between 2 and 4 to precachexia, a score between 4 and 8 to cachexia, and a score between 8 and 12 (maximal score) to refractory cachexia (details are described in the APPENDIX Table A1) (42). CRC Patients without cachexia met criteria of *1*) age $\geq$ 18 yr, *2*) no or minimal unintentional weight loss <2% or unintentional weight loss 2%–5% with BMI > 20 kg/m^2 or no sarcopenia, and *3*) CSS between 0 and 2. HCs were *1*) $\geq$ 18 yr old with *2*) BMI 18–30 kg/m^2. For all groups the exclusion criteria were identical: *1*) severe mental or psychological disorders, *2*) insufficient knowledge of the Dutch language, *3*) presence of muscle disorders influencing the spinal cord or lower limbs, and *4*) bedridden.

Sarcopenia was assessed in a subset of patients with CRC following the European Working Group on Sarcopenia in Older People (EWGSOP2) guidelines (40). Strength, assistance with walking, rising from a chair, climbing stairs, and falls (SARC-F) screening tool (scores $\leq$ 4 indicating symptomatic individuals) was followed by handgrip strength measurement (<27 kg men, <16 kg women), bioelectrical impedance analysis for lean mass (fat-free mass index <18 kg/m^2 men, <15 kg/m^2 women), and short physical performance battery (SPPB) test ($\leq$8 indicating reduced physical performance). Probable sarcopenia was defined by low strength, confirmed by low lean tissue mass, and severe sarcopenia by additional low SPPB score.

After meeting the inclusion criteria and obtaining written informed consent, all assessments were conducted at a single time point. In patients with CRC-associated cachexia, measurements were performed preoperatively in the following sequence: three-dimensional (3D) freehand ultrasound, SPPB test, handgrip strength assessment, questionnaires, and muscle biopsies under local anesthesia. The same assessments were performed with the HCs in the same order. In CRC patients without cachexia, the assessment protocol was identical, except that muscle biopsies were collected during surgery under general anesthesia.

The study was approved by the ethical committee of the Jessa Hospital Hasselt and Hasselt University (B2432021000037), and performed in accordance with the Declaration of Helsinki. All individuals gave written informed consent prior to the start of the study (registered at Clinicaltrials.gov; NCT number: NCT06780423).

Biopsy Procedure

Fine needle muscle biopsies were taken from the right *m. erector spinae* (in prone position) and *m. vastus lateralis* (in supine position) using a modified micro biopsy method described by Agten et al. (43). We chose to take biopsies from the *m. vastus lateralis* due to its association with functional outcomes and the *m. erector spinae* since it is the gold standard for clinically assessing skeletal muscle size and quality (8, 44). Samples were frozen in liquid nitrogen-cooled isopentane for immunohistochemistry and stored at −80°C.

Immunohistochemistry

Transverse cryosections (10 μm) obtained with the CM3050 cryostat (Leica Biosystems, Diegem, Belgium) were stained following the protocol of Betz et al. (45) with primary and the appropriate secondary antibodies for laminin, skeletal muscle fiber type I, capillaries, and myonuclei (details described in

the APPENDIX Table A2). Slides were mounted with ProLongTM Gold antifade mounting medium (Thermo Fisher Scientific). Images were captured at ×10 and ×20 magnification using an MC170 camera connected to a DM2000 LED microscope (Leica Biosystems). Images (×10 magnification) were analyzed using SMASH, a semiautomatic program, (MATLAB, MathWorks, MA), for fiber CSA, fiber type distribution, and the fiber relative CSA (RCSA). The fiber RCSA takes the number of each type of the muscle fibers and the fiber CSA into account and was calculated as follows:

$$\frac{\text{Mean CSA type I fibers} \times \text{Total type I fibers}}{(\text{Mean CSA type I fibers} \times \text{Total type I fibers}) + (\text{Mean CSA type II fibers} \times \text{Total type II fibers})}.$$

For these analyses, two to five fields of view were examined to ensure inclusion of a sufficient number of muscle fibers (*m. vastus lateralis*: 235 ± 72, *m. erector spinae*: 203 ± 49; Table 2). Muscle fiber myonuclei, myonuclear domain, and central nuclei were analyzed using ImageJ (×10 magnification; v1.54d software package, National Institute of Health, MD). For these analyses, only nuclei within the fiber boundary (laminin) were counted as myonuclei. One to three fields of view were examined to ensure inclusion of a sufficient number of muscle fibers (*m. vastus lateralis*: 129 ± 29, *m. erector spinae*: 121 ± 26; Table 2). Capillary density, capillary to fiber ratio, capillary domain, and heterogeneity index was analyzed using Btablet and AnaTis software (×20 magnification; BaLoH software, the Netherlands). For these analyses, two to five fields of view were examined to ensure inclusion of a sufficient number of muscle fibers (*m. vastus lateralis*: 104 ± 18, *m. erector spinae*: 101 ± 13; Table 3).

Freehand Ultrasound Image Acquisition and Processing

A 3D freehand ultrasound technique was applied to perform a longitudinal two- or three-sweep assessment of the *m. rectus femoris* in supine position with a knee roll placed under the participants popliteal. For the ultrasound assessment, the *m. rectus femoris*, part of the quadriceps muscles, was selected in preference of the *m. vastus lateralis*. This decision was based on the anatomical course of the *m. vastus lateralis*, which present challenges for consistent visualization using ultrasound imaging. The ultrasound device (EchoBlaster 128 CEXT-1Z, HL9.0/60/128Z-2 transducer, Telemed, Vilnius, Lithuania) was synchronized with a portable motion tracking system with three fixed optical cameras, a sampling rate of 120 Hz, and a spatial resolution of 1 mm (Optitrack V120: Trio, NaturalPoint). Four optical markers were mounted on the ultrasound transducer and tracked with the Optitrack V120. To integrate the two-dimensional (2D) ultrasound images with the positional information of the tracking system, we used Stradwin software (Mechanical Engineering, Cambridge University, UK) described by Rummens et al. (46). Muscle volume of the *m. rectus femoris* was determined using this method.

CT-Scan Analysis

Preoperative single slice CT-scans of CRC patients with and without cachexia were analyzed at the third lumbar vertebra (L3) level. Scans were analyzed using PACS (Sectra workstation IDS7, Linkoping, Sweden). CSA of the right-sided *m. erector spinae* was determined by manual planimetry using an area measurement tool. Besides CSA, muscle density was assessed based on the Hounsfield Units (HU),with higher HU values indicating a greater density and less fat infiltration and therefore a potential better quality of the muscle (47). Boundaries in HU for muscle tissue were set to −29 to +150 (48).

Physical Performance

To assess the physical performance of the subjects, the SPPB test was performed. This test comprises three subtests: a standing balance test, four-meter gait speed (4MGS), and five-times sit-to-stand (5STS). During the standing balance test, the patient had to maintain three stances (feet placed side by side, semi-tandem, tandem) for 10 s. The 4MGS was performed in duplicate to obtain habitual gait speed over 4 m. For the 5STS, the patient had to perform five sit-to-stand maneuvers as fast as possible with arms folded in front of their chest. Each subtest was scored on a scale from zero (extreme mobility impairment) to four (no mobility impairment), resulting in a total SPPB score ranging from 0 to 12, where higher scores indicate better physical function.

Handgrip strength was assessed using a JAMAR hydraulic dynamometer. Each subject performed three trials with their dominant hand, from which the highest strength value (in kg) was used for further analysis. During testing, subjects were seated comfortably, with the shoulder in an adducted position, the forearm in neutral rotation, and the elbow flexed at 90°.

Activity Pattern and Quality of Life

Physical Activity Scale for Individuals with Physical Disabilities.

Physical activity information was collected using the Physical Activity Scale for Individuals with Physical Disabilities (PASIPD) questionnaire, including different domains (leisure, household, and occupational activities). Patients were asked to recall the number of days in the past seven days that they participated in these activities [never, seldom (1–2 days/wk), sometimes (3–4 days/wk), or often (5–7 days/wk)] and on average how many hours a day they participated (<1, 1–2, 2–4, >4 h). The questionnaire consists of 12 items. The first item was included to familiarize with the item format and was therefore not scored. The remaining questions were filled in to obtain the total physical activity score, which was created by multiplying the average hours per day for each item by a metabolic equivalent (MET) value associated with the intensity of the activity (MET in h/day, maximum score is 182.3 MET h/day). One MET is defined

as the amount of oxygen required per minute under resting conditions (49).

36-item Short Form Survey.

The 36-item Short Form Survey (SF-36) questionnaire includes multiple subscales which are the following: physical functioning, role limitations due to physical health, role limitations due to emotional problems, energy/fatigue, emotional well-being, social functioning, pain, general health, and health change. The total score on each subscale ranges from 0 to 100. A greater score indicates a better perceived health and quality of life. Total score from the nine subscales can range from 0 to 900.

Statistical Analysis

JMP Pro 17.2 statistical software (SAS Campus Drive, Cary, NC) was used for the statistical analysis. Residuals were checked for normal distribution. A general linear model was used with group and sex as fixed effects and Student's *t* multiple comparisons tests were used for pairwise comparisons with Bonferroni correction. For Ordinal data (SPPB, SF-36, and PASIPD), the Kruskal-Wallis test was performed to test group differences. In case of significance, Wilcoxon each pair was used for pairwise comparisons with Bonferroni correction. Significance level of 0.05 was considered as statistically significant for main effects. Considering pairwise comparisons, an α level of 0.016 was applied based on Bonferroni correction (comparing three groups). Data are expressed as means ± standard deviation (SD).

Sample size estimates were based on previous data comparing skeletal muscle fiber CSA of the *m. vastus lateralis* in cachectic patients with lung cancer and HCs (20). Calculations indicated that 29 subjects per group were required to detect differences in type I muscle fiber CSA (effect size 0.66, $\alpha = 0.05$, $1 - \beta = 0.80$), and 9 subjects per group for type II muscle fiber CSA (effect size 1.26, $\alpha = 0.05$, $1 - \beta = 0.80$). Our study included 10 patients with CRC-associated cachexia, 25 CRC patients without cachexia, and 25 HCs. All groups exceeded the required sample size for type II muscle fiber CSA analysis. Post hoc achieved power analyses were performed for the different outcome measures (Gpower 3.1.9.7; APPENDIX Table A3).

RESULTS

Anthropometric Characteristics

A total of 12 patients with CRC-associated cachexia, 25 CRC patients without cachexia, and 25 HCs were included. Anthropometric data (Table 1) showed no significant differences in age, sex, body weight, length, and BMI ($P_{GROUP} > 0.05$, respectively). However, unlike the other groups, the CRC group with cachexia comprised more women than men. Cachexia staging scores differed significantly between CRC patients with and without cachexia ($P < 0.0001$). Tumor location and stage are detailed in APPENDIX Table A4.

Microscopic Skeletal Muscle Characteristics of the m. Vastus Lateralis

Representative *m. vastus lateralis* images for muscle fiber typing of HCs, and CRC patients with and without cachexia are shown in Fig. 1, *A–C*, respectively. CSA for type I muscle fibers did not differ between groups ($P_{GROUP} = 0.497$) (Fig. 1*D*, Table 2). In contrast, type II fiber CSA differed between groups ($P_{GROUP} = 0.033$), with a significantly smaller CSA in patients with CRC-associated cachexia (3,260 ± 860 μm^2) compared with HCs (4,773 ± 1,270 μm^2; $P = 0.009$) (Fig. 1*D*, Table 2). The proportion of type I ($P_{GROUP} = 0.036$) and type II muscle fibers ($P_{GROUP} = 0.036$) showed significant differences between groups. CRC patients without cachexia had proportionally fewer type I fibers (42 ± 14%; $P = 0.016$) and more type II fibers (58 ± 14%; $P = 0.016$) compared with HCs (type I: 52 ± 13%, type II: 48 ± 13%) (Fig. 1*E*, Table 2). No differences in RCSA for both type I and type II fibers were observed between groups ($P_{GROUP} = 0.090$, respectively) (Fig. 1*F*, Table 2).

The number of myonuclei per type I fiber ($P_{GROUP} < 0.001$) and type II fiber ($P_{GROUP} < 0.001$) differed between groups. The number of myonuclei was significantly reduced in both fiber types in CRC patients with cachexia (type I: 3.12 ± 1.03; $P < 0.001$, type II: 2.48 ± 1.07; $P = 0.001$) and without cachexia (type I: 3.54 ± 1.18; $P < 0.001$, type II: 3.07 ± 1.08; $P = 0.001$) compared with HCs (type I: 4.71 ± 0.92, type II: 4.17 ± 1.16) (Fig. 1*G*, Table 2). The myonuclear domain of type I fibers differed between groups ($P_{GROUP} = 0.003$), with a significant increase in patients with CRC-associated cachexia (1,890 ± 761 μm^2) compared with HCs (1,243 ± 237 μm^2; $P = 0.001$). The myonuclear domain of type I fibers only tended to be increased in CRC patients without cachexia compared with HCs ($P = 0.038$). For type II fibers, the myonuclear domain did not differ between groups ($P_{GROUP} = 0.063$)(Fig. 1*H*, Table 2). Interestingly, there was no difference between groups in central nuclei, neither for type I ($P_{GROUP} = 0.135$) nor for type II fibers ($P_{GROUP} = 0.362$) (Fig. 1*I*, Table 2).

Capillary-to-fiber (C:F) ratio did not differ between groups ($P_{GROUP} = 0.118$) (Fig. 1*J*, Table 3). Capillary fiber

Table 1. *Anthropometric data*

	Healthy Controls ($n = 25$)	CRC Patients without Cachexia ($n = 25$)	Patients with CRC-Associated Cachexia ($n = 12$)	P_{GROUP}
Age, yr (age range)	66 ± 10 (41–81)	66 ± 13 (39–86)	66 ± 15 (43–88)	0.988
Sex (male:female)	18:7	18:7	5:7	0.142
Body weight, kg	78.8 ± 11.5	82.7 ± 15.2	75.6 ± 16.1	0.321
Length, m	1.73 ± 0.07	1.76 ± 0.08	1.71 ± 0.07	0.104
Body mass index, kg/m^2	26.2 ± 2.6	26.5 ± 3.5	25.9 ± 5.1	0.887
Cachexia staging score (0–12)	NA	1 ± 1	6 ± 1	**<0.0001**

Values are presented as means ± SD, range or number only. $P < 0.05$ in bold. CRC, colorectal cancer.

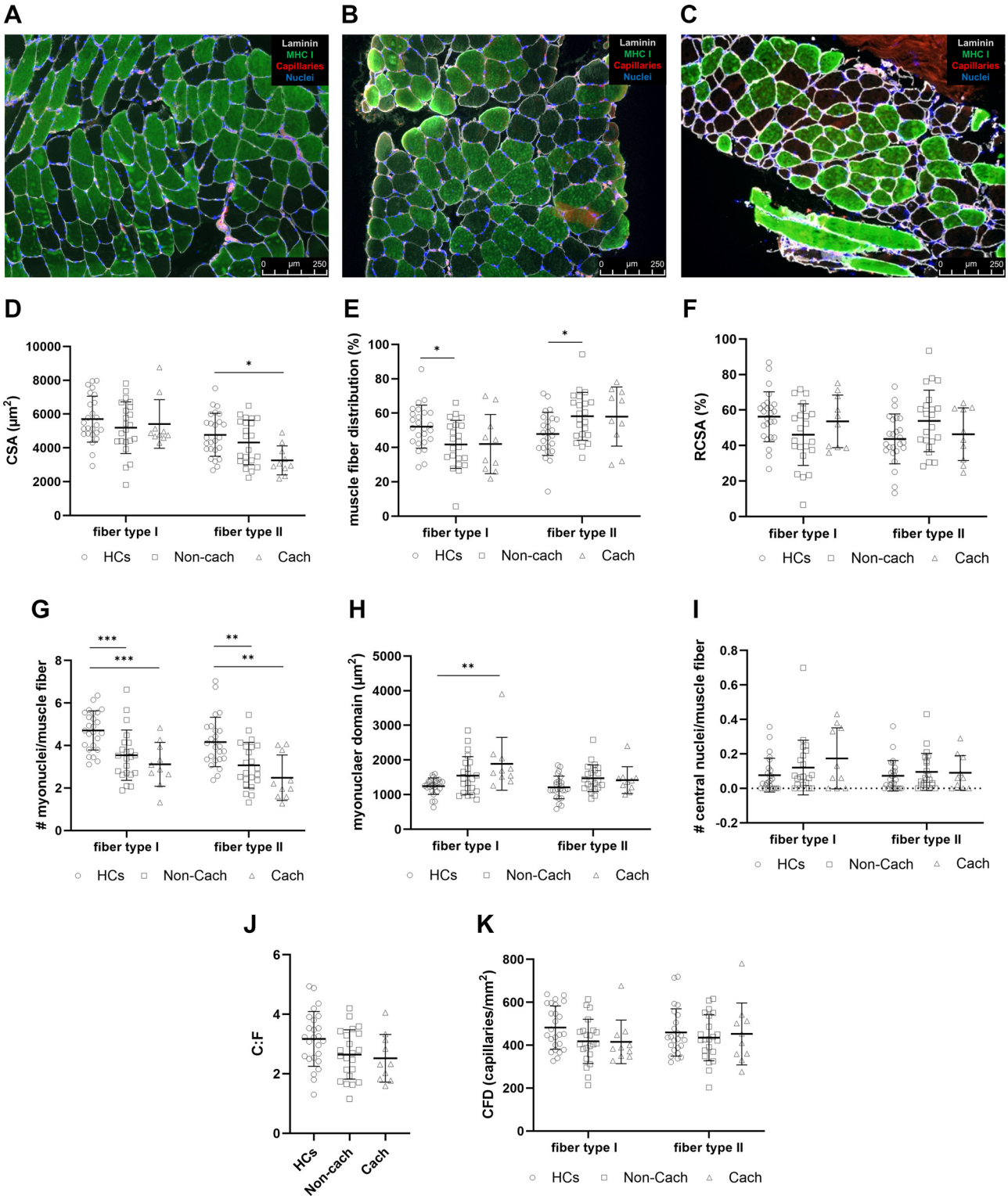

Figure 1. Skeletal muscle characteristics of the *m. vastus lateralis*. Representative immunofluorescence images of healthy control (HC; *A*), patients with colorectal cancer (CRC) without cachexia (*B*), and patients with CRC-associated cachexia (*C*) muscle biopsies stained for laminin (gray), myosin heavy chain (MHC) I (green), nuclei/DAPI (blue), and capillaries/CD31 (red). HCs (○, $n = 25$), CRC patients without cachexia (□, $n = 22$), and patients with CRC-associated cachexia (△, $n = 10$). Quantitative analyses include: muscle fiber cross-sectional area (CSA) (*D*), fiber type distribution (*E*), relative CSA (*F*), number of myonuclei per fiber (*G*), myonuclear domain (*H*), number of central nuclei per fiber (*I*), capillary-to-fiber ratio (C:F; *J*), and capillary fiber density (CFD; *K*). Data are presented as individual values with means ± SD. *$P < 0.016$, **$P < 0.005$, ***$P < 0.001$. noncach, noncachectic; cach, cachectic; RCSA, relative cross-sectional area; SD, standard deviation.

Table 2. *Microscopic skeletal muscle characteristics of the* m. vastus lateralis *and* m. erector spinae

Muscle Fiber Type	Healthy Controls	CRC Patients without Cachexia	Patients with CRC-Associated Cachexia
m. vastus lateralis	$n = 25$	$n = 22$	$n = 10$
Number of muscle fibers counted	202 ± 48	269 ± 78	244 ± 74
CSA, μm^2			
Type I	5,703 ± 1,359	5,197 ± 1,531	5,415 ± 1,438
Type II	4,773 ± 1,270	4,322 ± 1,322	3,260 ± 860*
%			
Type I	52 ± 13	42 ± 14*	42 ± 17
Type II	48 ± 13	58 ± 14*	58 ± 17
RCSA, %			
Type I	56 ± 14	46 ± 17	54 ± 15
Type II	44 ± 14	54 ± 17	46 ± 15
Number of muscle fibers counted	126 ± 28	131 ± 30	133 ± 33
Number myonuclei/fiber			
Type I	4.71 ± 0.92	3.54 ± 1.18*	3.12 ± 1.03*
Type II	4.17 ± 1.16	3.07 ± 1.08*	2.48 ± 1.07*
Myonuclear domain, μm^2			
Type I	1,243 ± 237	1,550 ± 547	1,890 ± 761*
Type II	1,209 ± 327	1,473 ± 389	1,418 ± 387
Number central nuclei/fiber			
Type I	0.08 ± 0.10	0.12 ± 0.16	0.17 ± 0.18
Type II	0.07 ± 0.09	0.10 ± 0.11	0.09 ± 0.10
m. erector spinae	$n = 23$	$n = 20$	$n = 10$
Number of muscle fibers counted	207 ± 45	202 ± 54	198 ± 54
CSA, μm^2			
Type I	6,325 ± 1,611	6,296 ± 2,344	5,124 ± 1,515
Type II	5,234 ± 1,396	5,465 ± 1,797	4,671 ± 2,259
%			
Type I	68 ± 11	57 ± 15*	58 ± 15
Type II	32 ± 11	43 ± 15*	42 ± 15
RCSA, %			
Type I	72 ± 11	60 ± 17*	61 ± 19
Type II	28 ± 11	40 ± 17*	39 ± 19
Number of muscle fibers counted	122 ± 26	121 ± 26	122 ± 30
Number myonuclei/fiber			
Type I	4.66 ± 0.99	4.34 ± 1.46	3.58 ± 1.02
Type II	3.63 ± 1.31	3.23 ± 1.33	2.39 ± 1.19
Myonuclear domain, μm^2			
Type I	1,386 ± 358	1,472 ± 286	1,482 ± 392
Type II	1,535 ± 475	1,790 ± 469	2,080 ± 718
Number central nuclei/fiber			
Type I	0.11 ± 0.08	0.33 ± 0.46	0.27 ± 0.33
Type II	0.10 ± 0.14	0.12 ± 0.12	0.19 ± 0.21

Values are presented as means ± SD. CRC, colorectal cancer; CSA, cross-sectional area; m., muscle; RCSA, relative cross-sectional area. *$P < 0.05$ compared with the healthy control group.

density (CFD) did not differ between groups for both type I ($P_{GROUP} = 0.101$) and type II fibers ($P_{GROUP} = 0.778$) (Fig. 1*K*, Table 3). The capillary domain ($P_{GROUP} = 0.165$) and heterogeneity index ($P_{GROUP} = 0.409$) did not differ between groups (Table 3).

Microscopic Skeletal Muscle Characteristics of the m. Erector Spinae

Representative *m. erector spinae* images for muscle fiber typing of HCs, and CRC patients without cachexia and with cachexia are shown in Fig. 2, *A*–*C*, respectively. There were no significant differences in the mean CSA of type I ($P_{GROUP} = 0.538$) nor type II fibers ($P_{GROUP} = 0.699$) between groups (Fig. 2*D*, Table 2). A significant difference in the proportion of type I ($P_{GROUP} = 0.033$) and type II fibers ($P_{GROUP} = 0.033$) between groups has been observed, with CRC patients without cachexia showing proportionally fewer type I fibers (57 ± 15%; $P < 0.012$) and more type II fibers (43 ± 15%; $P < 0.012$) compared with HCs (type I: 68 ± 11%, type II: 32 ± 11%) (Fig. 2*E*, Table 2). As such, significant differences were observed between groups for the RCSA of type I and type II fibers ($P_{GROUP} = 0.035$, respectively). The RCSA of type I fibers was lower in CRC patients without cachexia (60 ± 17%; $P = 0.013$), whereas RCSA of type II fibers was higher in CRC patients without cachexia (40 ± 17%; $P = 0.013$) compared with HCs (type I: 72 ± 11%, type II: 28 ± 11%) (Fig. 2*F*, Table 2).

No differences between groups were observed for the number of myonuclei per type I ($P_{GROUP} = 0.212$) and type II fiber ($P_{GROUP} = 0.187$) (Fig. 2*G*, Table 2). The myonuclear domain did not differ between groups for type I ($P_{GROUP} = 0.547$) and type II fibers ($P_{GROUP} = 0.061$) (Fig. 2*H*, Table 2). Furthermore, the number of central nuclei per type I ($P_{GROUP} = 0.103$) and type II fiber ($P_{GROUP} = 0.250$) were similar between groups (Fig. 2*I*, Table 2).

The C:F ratio showed no differences between groups ($P_{GROUP} = 0.846$) (Fig. 2*J*, Table 3). The CFD of type I fibers differed between groups ($P_{GROUP} = 0.049$). However, post hoc pairwise comparisons showed only an approached significance toward a higher CFD of type I fibers in patients with CRC-associated cachexia (385.21 ± 113.49 capillaries/

Table 3. *C:F, CFD for type I and II fibers, capillary domains, and heterogeneity index of the* m. vastus lateralis *and* m. erector spinae

	C:F	CFD Type I, capillaries/mm²	CFD Type II, capillaries/mm²	Capillary Domain, µm²	Heterogeneity Index (LogSD)
m. vastus lateralis					
Number of muscle fibers counted (healthy controls: 109 ± 13, CRC patients without cachexia: 98 ± 23, patients with CRC-associated cachexia: 103 ± 12)					
Healthy controls ($n = 25$)	3.17 ± 0.92	482.61 ± 100.68	459.43 ± 109.99	2,279 ± 492	0.21 ± 0.02
CRC patients without cachexia ($n = 22$)	2.65 ± 0.83	418.03 ± 102.98	435.24 ± 107.24	2,615 ± 705	0.21 ± 0.02
Patients with CRC-associated cachexia ($n = 10$)	2.52 ± 0.80	415.76 ± 101.39	452.72 ± 144.08	2,513 ± 605	0.21 ± 0.02
m. erector spinae					
Number of muscle fibers counted (healthy controls: 102 ± 14, CRC patients without cachexia: 98 ± 11, patients with CRC-associated cachexia: 105 ± 14)					
Healthy controls ($n = 23$)	2.92 ± 1.09	386.58 ± 123.00	358.49 ± 115.47	2,987 ± 1086	0.22 ± 0.02
CRC patients without cachexia ($n = 20$)	2.92 ± 1.01	322.58 ± 85.68	301.41 ± 76.71	3,534 ± 969	0.23 ± 0.03
Patients with CRC-associated cachexia ($n = 10$)	2.37 ± 0.77	385.21 ± 113.49	387.35 ± 108.87#	3,174 ± 767	0.22 ± 0.02

Values are presented as means ± SD. C:F, capillary to fiber ratio; CFD, capillary fiber density; CRC, colorectal cancer; m., muscle; SD, standard deviation. #$P < 0.05$ compared with the noncachectic CRC group.

mm²) compared with CRC patients without cachexia (322.58 ± 85.68 capillaries/mm²; $P = 0.028$) (Fig. 2*K*, Table 3). The CFD of type II fibers also differed between groups ($P_{GROUP} = 0.030$), with an increase in patients with CRC-associated cachexia (387.35 ± 108.87 capillaries/mm²) compared with CRC patients without cachexia (301.41 ± 76.71 capillaries/mm²; $P = 0.012$) (Fig. 2*K*, Table 3). The capillary domain ($P_{GROUP} = 0.166$) and heterogeneity index ($P_{GROUP} = 0.689$) showed no differences between groups (Table 3).

Macroscopic Skeletal Muscle Characteristics and Volume

CT scans showed no significant difference for absolute CSA of the *m. erector spinae* between patients with CRC-associated cachexia (1788 ± 447 mm²) and CRC patients without cachexia (2105 ± 417 mm²; $P = 0.146$) (Fig. 3*A*, Table 4), irrespective of body height normalization ($P = 0.139$) (Fig. 3*B*, Table 4). Skeletal muscle density [expressed as Hounsfield Unit (HU)] was significantly lower in patients with CRC-associated cachexia (21 ± 25) compared with CRC patients without cachexia (38 ± 10; $P = 0.031$) (Fig. 3*C*, Table 4).

Of interest, muscle fiber CSA of the *m. vastus lateralis* ($r = 0.61$; $P = 0.0003$) and *m. erector spinae* ($r = 0.50$; $P = 0.006$) correlated positively with CT-based CSA of the *m. erector spinae* (Fig. 4, *A* and *B*). In addition, ultrasound-based volume of the *m. rectus femoris* showed a significant difference between groups ($P_{GROUP} = 0.031$). Here, *m. rectus femoris* volume was significantly lower in patients with CRC-associated cachexia (69 ± 32 mL) compared with HCs (104 ± 41 mL; $P = 0.010$), while only tending to be decreased compared with CRC patients without cachexia (96 ± 32 mL; $P = 0.039$) (APPENDIX Fig. A1).

Muscle Strength, Physical Functioning, Physical Activity, and Quality of Life

Performance of the SPPB test differed between groups ($P_{GROUP} = 0.002$), where both CRC groups scored worse (CRC patients without cachexia: 10.2 ± 2.3; $P = 0.013$, patients with CRC-associated cachexia: 9.1 ± 2.2; $P < 0.001$) compared with HCs (11.4 ± 0.9). This mainly manifested in a tendency toward a poorer performance in the 4-m walk test ($P_{GROUP} = 0.070$) and a worse performance on the five-times sit-to-stand test ($P_{GROUP} = 0.001$) (Table 5). Both patients group with CRC scored significantly lower on the five-times sit-to-stand test (cachexia: 2.2 ± 1.2; $P < 0.001$, noncachexia: 2.8 ± 1.1; $P = 0.004$) compared with HCs (3.6 ± 0.8) (Table 5). No differences between groups were observed for the balance test ($P_{GROUP} = 0.379$) (Table 5). Handgrip strength did not differ between groups ($P_{GROUP} = 0.151$) (Table 5).

Of interest, skeletal muscle density (HU) positively correlated with total SPPB score ($r = 0.47$; $P = 0.004$). Muscle fiber CSA of the *m. vastus lateralis* positively correlated with handgrip strength ($r = 0.59$; $P < 0.001$), as was true for CT-based CSA of the m. erector spinae ($r = 0.53$; $P = 0.001$) (Fig. 4, *C*–*E*).

No differences were observed between groups for physical activity behavior ($P_{GROUP} = 0.412$) (Table 5). The total score on the SF-36 differed between groups ($P_{GROUP} = 0.005$), where both CRC patients with and without cachexia had lower total SF-36 scores (cachexia: 555.8 ± 156.9; $P = 0.003$, noncachexia: 622.9 ± 137.4; $P = 0.013$) compared with HCs (719.0 ± 86.7) (Table 5). In the subcategories of the SF-36, differences between groups were found for "limitations due to physical health" ($P_{GROUP} = 0.032$), "limitations due to emotional problems" ($P_{GROUP} = 0.031$), and "health change" ($P_{GROUP} = 0.009$). Specifically, patients with CRC-associated cachexia scored significantly lower compared with HCs in limitations due to physical health (cachexia: 50.0 ± 39.1, HCs: 85.5 ± 29.24; $P = 0.007$), limitations due to emotional problems (cachexia: 66.7 ± 35.1, HCs: 94.7 ± 16.7; $P = 0.006$), and health change (cachexia: 32.5 ± 12.1, HCs: 50.0 ± 8.3; $P < 0.001$) (APPENDIX Fig. A2). Of interest, correlation analyses showed a significant positive association between total SF-36 score and CT-scan CSA of the *m. erector spinae* ($r = 0.54$; $P = 0.001$) (Fig. 4*F*).

DISCUSSION

This study demonstrates insights into macro- and microscopic skeletal muscle characteristics and their associations with clinical measures of physical functioning in CRC patients with and without cachexia. Skeletal muscle-specific alterations in microscopic *m. vastus lateralis* fiber CSA and

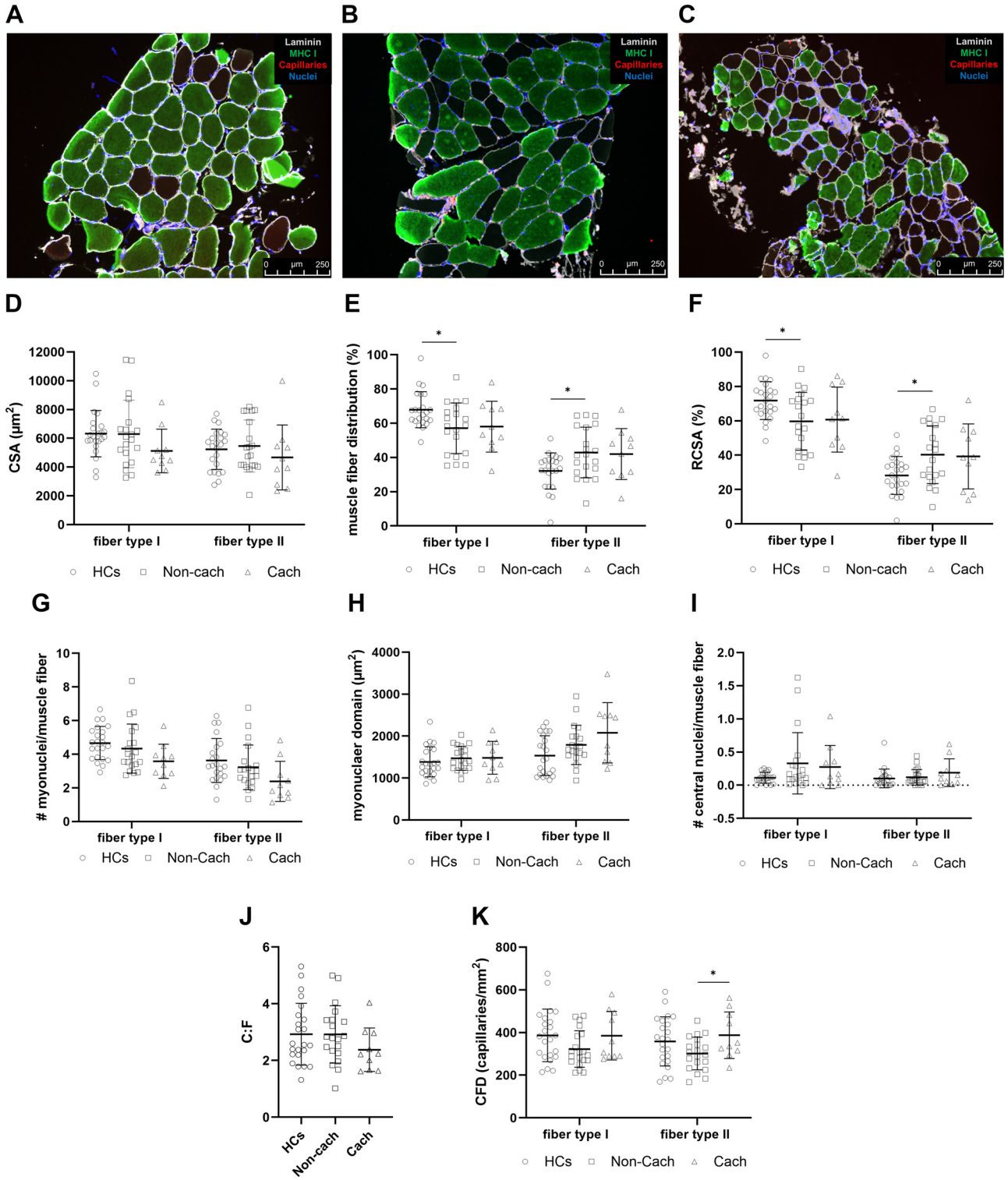

Figure 2. Skeletal muscle characteristics of the *m. erector spinae*. Representative immunofluorescence images of healthy control (HC; *A*), patients with colorectal cancer (CRC) without cachexia (*B*), and patients with CRC-associated cachexia (*C*) muscle biopsies stained for laminin (gray), myosin heavy chain (MHC) I (green), nuclei/DAPI (blue), and capillaries/CD31 (red). HCs (○, $n = 23$), CRC patients without cachexia (□, $n = 20$), and patients with CRC-associated cachexia (△, $n = 10$). Quantitative analyses include: muscle fiber cross-sectional area (CSA) (*D*), fiber type distribution (*E*), relative CSA (*F*), number of myonuclei per fiber (*G*), myonuclear domain (*H*), number of central nuclei per fiber (*I*), capillary-to-fiber ratio (C:F; *J*), and capillary fiber density (CFD; *K*). Data are presented as individual values with means ± SD. *$P < 0.016$. noncach, noncachectic; cach, cachectic; RCSA, relative cross-sectional area; SD, standard deviation.

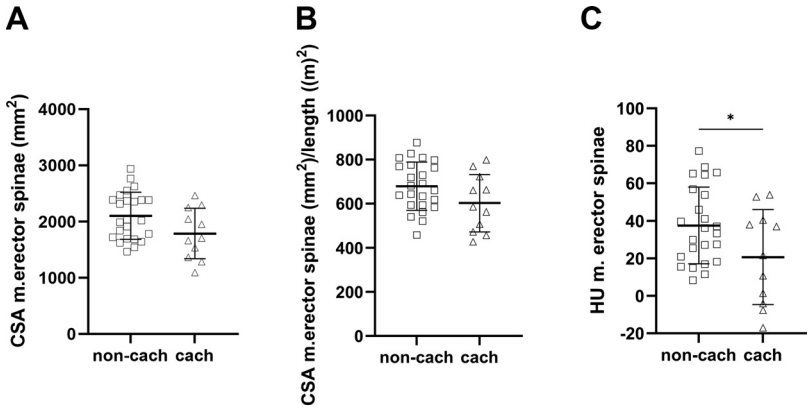

Figure 3. Muscle mass and quality of the *m. erector spinae*. Mean cross-sectional area (CSA) (*A*), mean CSA corrected for body height (*B*), and muscle quality (*C*) (Hounsfield Units, HU) of the *m. erector spinae* in patients with colorectal cancer (CRC) without cachexia (□, $n = 24$) and with cachexia (△, $n = 11$). Data are presented as individual values and means ± SD. *$P < 0.05$. noncach, noncachectic; cach, cachectic; SD, standard deviation.

myonuclear content, and *m. erector spinae* capillarization were found in patients with CRC. Furthermore, we observe a significant reduction in CT-based muscle density and a reduced volume of the *m. rectus femoris* in CRC patients with cachexia. Of interest, clinically highly relevant correlations between microscopic skeletal muscle alterations, macroscopic skeletal muscle alterations, muscle functioning, and quality of life were observed, postulating that in clinical practice preoperative CT-scans could serve as an important source of information on skeletal muscle tissue characteristics, potentially being a base for optimized patient management and quality of life.

The selective atrophy of type II muscle fibers observed in the *m. vastus lateralis* of CRC patients with cachexia in our study is supported by several preclinical and clinical findings. Studies on CC in animal models for peritoneal carcinomatosis (22) and CRC (23, 24), and in patients with lung (25), gastric, pancreatic, and colon cancer (26), have reported preservation of type I fiber CSA and predominant atrophy of type II fibers. However, the fiber type-specific atrophy has not been corroborated by others, where overall muscle fiber atrophy in CC has been suggested in both preclinical animal models [pancreatic cancer (50), lung cancer (16–18), and CRC (19, 51)] and clinical studies including gastrointestinal (21, 52) and with lung cancer (20). Furthermore, we observe a shift toward a higher proportion of type II fiber in CRC patients without cachexia compared with HCs, but not in patients with CRC-associated cachexia when corrected for sex. This is in line with preclinical animal models (53–56) and former clinical studies showing no differences in muscle fiber type distribution between patients with CC and healthy individuals (25, 26) or when compared with noncachectic cancer patients (20, 21, 28). In contrast, another study including cachectic patients with colon, pancreatic, and gastric cancer showed a shift toward type II fibers (27).

These inconsistencies in results between studies may reflect differences in cancer type, disease stage, muscle groups examined, and diagnostic or staging criteria for CC. Sun et al. (57) showed differences in early CC and late CC in mice, with the latter showing significantly more reduction in skeletal muscle fiber CSA. Of interest, Op den Kamp et al. (20) reported nonselective fiber atrophy in patients with advanced stage lung cancer without a shift in fiber composition, whereas our cohort also included patients with earlier stage of CRC. In addition, diagnostic criteria for CC varied across studies. Notably, Johns et al. (21) found that only patients with both low muscularity and weight loss showed atrophy in both fiber types, whereas other classifications showed no change or selective type II fiber atrophy. Therefore, it is tempting to speculate that looking at earlier staging of cachexia shows only type II fiber specific atrophy, with type I fibers being more likely to be affected only in later and more severe stages of cachexia (such as in refractory-cachexia). This could explain why we only observe atrophy of type II muscle fibers as we only included CRC patients with cachexia in the cachectic stage (CCS score between five and eight).

The observed reduction in the number of myonuclei per type I and type II muscle fiber of the *m. vastus lateralis*, observed in both CRC patients with and without cachexia, corresponds with previous studies indicating that muscle atrophy is accompanied by a decrease in myonuclear content (29, 58). Here, an increase in the myonuclear domain of type I fibers in patients with CRC-associated cachexia was observed, potentially resulting from a decrease in numbers of myonuclei per fiber in the cachectic group, irrespective of the number of central nuclei. Some previous studies, however, did show a small, but significant increase in central nuclei in patients with pancreatic cachexia (59) and CRC cachexia (60), as well as in animal models of CC (16, 61). As central nuclei are typically indicative of ongoing muscle regeneration, existing literature suggests that muscle regeneration is impaired in CC due to the inhibition of satellite cell differentiation (62). Moreover, Daou et al. (30) shows the presence of central nuclei in muscle fibers of cachectic

Table 4. *Macroscopic skeletal muscle cross-sectional area and density (Hounsfield Units) of the* m. erector spinae

	CSA, mm²	CSA, mm²/Patient Body Height², m²	HU
Patients with CRC-associated cachexia	1,788 ± 447	603 ± 129	21 ± 25#
CRC patients without cachexia	2,105 ± 417	679 ± 109	38 ± 10

Values are presented as means ± SD. CRC Patients with cachexia ($n = 11$) and without cachexia ($n = 24$). CRC, colorectal cancer; CSA, cross-sectional area; HU, Hounsfield units; m., muscle. #$P < 0.05$ compared with the noncachectic CRC group.

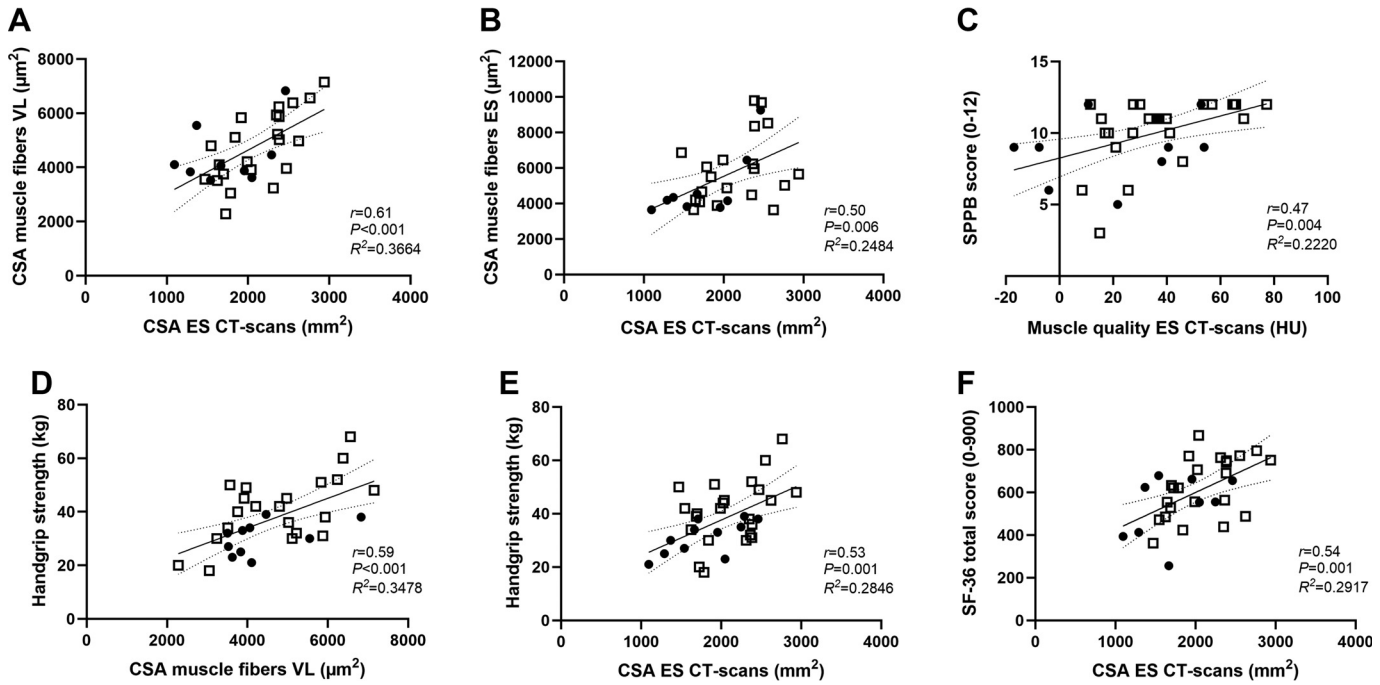

Figure 4. Correlation analyses between microscopic and macroscopic muscle characteristics and physical performance measures. ●, patients with colorectal cancer (CRC)-associated cachexia and □, CRC patients without cachexia. *A*: correlation between muscle fiber CSA of the vastus lateralis muscle and cross-sectional area (CSA) of the erector spinae muscle on, computed tomography (CT) scans at level lumbar 3 (cach $n = 9$, noncach $n = 22$). *B*: correlation between muscle fiber CSA of the erector spinae muscle and CSA of the erector spinae muscle on CT scans at level lumbar 3 (cach $n = 9$, noncach $n = 20$). *C*: correlation between the muscle quality (Hounsfield Units, HU) of the erector spinae muscle on CT scans at level lumbar 3 and the Short Physical Performance Battery (SPPB) test (cach $n = 10$, noncach $n = 24$). *D*: correlation between muscle fiber CSA of the vastus lateralis muscle and the handgrip strength (cach $n = 10$, noncach $n = 21$). *E*: correlation between the CSA of the erector spinae muscle on CT scans at level lumbar 3 and the handgrip strength (cach $n = 11$, noncach $n = 23$). *F*: correlation between the CSA of the erector spinae muscle on CT scans at level lumbar 3 and patient's quality of life (cach $n = 9$, noncach $n = 23$). All graphs are presented with a linear regression line with 95% confidence bands, *r* value, *P* value, and *R* squared value. cach, cachectic; ES, erector spinae; noncach, noncachectic; VL, vastus lateralis.

patients with gastrointestinal cancer and C26 mice alongside increased expression of markers associated with denervation and motor neuron loss. These findings suggest that the presence of central nuclei in CC may reflect a denervation-related process rather than a regenerative response to myofiber damage (30).

Adequate muscle tissue perfusion is critical in muscle mass maintenance, as it is essential for oxygen, nutrients, and growth factors delivery to the muscle (63). No differences in C:F ratio were observed within the different muscles studied here. In contrast, a previous study reported reduced muscle vascularization in cachectic patients with breast cancer (64). Capillary fiber density remained unchanged in the *m. vastus lateralis*, which can be explained by the reduced CSA of type II muscle fibers, reflecting findings in cachectic patients with upper gastrointestinal cancer (65). However, further research looking into the different subtypes of type II muscle fibers could provide additional valuable insights about shifts in muscle fiber phenotyping and capillary fiber density, as these fiber subtypes are suggested to differ metabolically (66), although the existence has been questioned recently (67).

Table 5. *Short physical performance battery test, handgrip strength, Physical Activity Scale for Individuals with Physical Disabilities, and 36-item Short Form Survey*

	Healthy Controls	Non-Cachectic	Cachectic	P_{GROUP}
SPPB total score (0–12)	11.4 ± 0.9	10.2 ± 2.3*	9.1 ± 2.2*	0.002
Walk speed (0–4)	3.8 ± 0.4	3.5 ± 0.8	3.2 ± 0.9	0.070
Sit-to-stand (0–4)	3.6 ± 0.8	2.8 ± 1.1*	2.2 ± 1.2*	0.001
Balance (0–4)	3.9 ± 0.2	3.7 ± 0.6	3.6 ± 0.8	0.379
Handgrip strength, kg	41.7 ± 11.9	41.3 ± 11.5	31.2 ± 6.0	0.151
PASIPD, MET h/day	20.2 ± 11.4	17.7 ± 14.5	16.8 ± 13.8	0.412
SF-36 total score (0–900)	719.0 ± 86.7	622.9 ± 137.4*	555.8 ± 156.9*	0.005

Values are presented as means ± SD. SPPB: healthy controls $n = 21$, noncachectic $n = 25$, cachectic $n = 11$. Handgrip strength: healthy controls $n = 24$, noncachectic $n = 24$, cachectic $n = 12$. PASIPD: healthy controls $n = 25$, noncachectic $n = 24$, cachectic $n = 12$. SF-36: healthy controls $n = 19$, noncachectic $n = 24$, cachectic $n = 10$. MET, metabolic equivalent; PASIPD, Physical Activity Scale for Individuals with Physical Disabilities; SF-36, 36-item Short Form Survey; SPPB, Short Physical Performance Battery Test.*Significantly different compared with healthy controls.

At the macroscopic level, patients with CRC-associated cachexia had lower muscle volume (*m. rectus femoris*), although similar CSA of the *m. erector spinae* were observed after correction for sex. Therefore, our CT-based findings for CSA do not align with existing literature, using CT- or MRI-based skeletal muscle quantification, demonstrating muscle wasting in patients with CC, likely being associated with disease severity and cachexia status (8, 68–70). However, the observed decline in muscle density (lower HU values) further supports the notion that CC is characterized not only by muscle atrophy but also by qualitative changes such as increased fat infiltration and fibrosis (8, 71, 72). Notably, our study shows that a microscopic lower CSA of the *m. vastus lateralis* and *m. erector spinae* muscle fibers correlates with a reduced macroscopic CT-based CSA of the *m. erector spinae*, which could have significant implications for clinical practice. This association suggests that routinely preoperative CT-scans may serve not only for anatomical assessment and staging of the tumor, but could also serve as a noninvasive surrogate marker for skeletal muscle quantity and quality in patients with (cachectic) cancer. This could enable earlier identification of patients at risk for developing cachexia or poor postoperative outcomes since muscle function and quality are critical determinants of recovery, treatment tolerance, and overall survival in patients with cancer (2, 73, 74). If CT-derived muscle metrics are validated as surrogate markers of microscopic muscle characteristics, they may pave the way for personalized prehabilitation strategies. Patients demonstrating diminished muscle CSA or attenuation on CT-scans could be stratified toward tailored intervention, including nutritional optimization, resistance and/or aerobic conditioning, prior to major oncologic therapy or surgery. Such an approach has the potential to enhance functional reserve, mitigate perioperative morbidity, and favorably modify disease management for patients with CRC.

In our study cohort, functional consequences of muscle wasting were evident, as patients with CRC cachexia exhibited reduced physical performance by using the SPPB test, reinforcing previous findings that CC impairs muscle function (37, 75, 76). Although our findings suggest similar handgrip strength among groups, at least partly explained by different sex distribution between our relatively small study groups, another human study found reduced handgrip strength in cachectic patients with advanced cancer (stage III and IV) compared with noncachectic cancer patients and HCs (75). Of interest, Delfinis et al. (51) showed that reduction in muscle force occurs prior to atrophy of the muscles, suggesting that muscle weakness occurs already in the precachectic stage of the C26 mice model. These discrepancies may be attributable to differences in the voluntary nature of clinical handgrip strength assessments, in contrast to involuntary contractions in preclinical models (51). Notably, the observed lower SPPB scores in both CRC patients with and without cachexia compared with HCs corroborate the (early) presence of muscle dysfunction in patients with cancer regardless of cachexia or muscle atrophy status (77, 78). Furthermore, we show significant positive correlations between handgrip strength and both micro- and macroscopic skeletal muscle CSA, as well as a positive correlation between functional performance measures (i.e., SPPB test) and macroscopic muscle density. This aligns with existing literature indicating that reductions in muscle mass, as we observe in our micro- and macroscopic skeletal muscle alterations, are associated with muscle weakness and increased muscular fatigability, all of which may contribute to a diminished quality of life of the patient (79, 80). Indeed, quality of life was markedly reduced in patients with CRC, particularly those with cachexia, emphasizing muscle dysfunction as a determinant of poor quality of life (81–84). Consistent with this, our data demonstrate a positive association between SF-36 scores and CT-derived CSA of the *m. erector spinae*, indicating that reduced muscle mass correlates with impaired quality of life. These findings highlight the potential of preoperative CT-based muscle assessment as a predictor of patient reported outcomes.

Interestingly, physical activity levels did not differ between groups based on PASIPD. This contrasts with prior reports of reduced activity in patients with CC, likely due to methodological differences (84–86). Although our study used a self-reported questionnaire, others use accelerometer techniques which are more objective and less prone to bias.

Study Limitations

Although this study provides important insights, some limitations should be acknowledged. One limitation of the present study is the relatively small sample size of the cachectic CRC group that may have constrained our ability to detect more subtle differences, especially for microscopic characteristics. Post hoc power analyses were performed showing low statistical power for some outcome measurements. Details are listed in APPENDIX Table A3 (G*Power 3.1.9.7).

Furthermore, the cachectic CRC group was not matched for sex with the noncachectic CRC group and HCs. Although no statistically differences were observed in this variable, potential residual confounding factors cannot be ruled out. As age and sex are known to play a role in skeletal muscle fiber CSA and contractile performance (87–90), we corrected for sex in our statistical analyses.

In addition, the cross-sectional design of this study limits causal inferences. Future longitudinal studies are warranted to investigate the temporal progression of muscle alterations in patients with CRC-associated cachexia and to explore the efficacy of potential therapeutic interventions, including exercise and nutritional support, to mitigate muscle wasting in cancer.

Conclusions

This study delineates both micro- and macroscopic alterations in skeletal muscle associated with cachexia in patients with CRC. At the microscopic level, patients with CRC-associated cachexia showed a marked reduction in muscle fiber type II CSA, a decrease in myonuclear content, and an expansion of the myonuclear domain. At the macroscopic level, these patients demonstrated a significant reduction in overall CT-derived muscle density and a reduced muscle volume of the *m. rectus femoris*.

Our findings indicate that macroscopic CT-based measures of muscle loss are correlated with microscopic alterations in skeletal muscle, supporting potential utility of

preoperative CT imaging-scans as a surrogate marker for muscle characteristics and quality in patients with CRC. The decline in muscle function and physical performance underscores the clinical relevance of these micro- and macroscopic alterations, emphasizing the contribution of muscle dysfunction and reduced muscle mass to impaired quality of life. This was further substantiated by our observation of a positive association between patient-reported quality of life and CT-based CSA of the *m. erector spinae*. Furthermore, micro- and macroscopic skeletal muscle alterations were associated with impaired physical function.

Despite inherent study limitations, these results emphasize the need for further investigation. Future longitudinal studies should delineate the temporal progression of muscle alterations and assess the efficacy of targeted interventions, including nutritional support and structured exercise programs, to mitigate muscle wasting and optimize patient outcomes.

APPENDIX

This appendix provides additional details on the methods (APPENDIX Tables A1, A2, and A3), tumor characteristics (APPENDIX Table A4), and results (APPENDIX Figs. A1 and A2). The Cachexia Staging Score was used as an inclusion criterium for patients with colorectal cancer (APPENDIX Table A1). Immunohistochemistry was used to perform fluorescent staining of skeletal muscle fibers, with primary and secondary antibodies listed in APPENDIX Table A2. Due to the smaller sample size of the cachectic cancer group compared with other groups, post hoc power calculations were conducted for all outcome measures (APPENDIX Table A3). Tumor location and staging data were collected from all patients with cancer (APPENDIX Table A4).

Additional details on the results are presented in APPENDIX Figs. A1 and A2. The muscle volume of the *m. rectus femoris* was assessed using the 3DfUS (APPENDIX Fig. A1). APPENDIX Figure A2 shows the SF-36 scores about the quality of life.

Table A1. *Cachexia staging score*

Measurements	Value	Score
Weight loss last 6 mo	Weight is stable or gained weight	0
	Weight loss $\leq$ 5%	1
	Weight loss $\geq$ 5% and $\leq$ 15%	2
	Weight loss $\geq$ 15%	3
Strength, Assistance with walking, Rise from a chair, Climb stairs, and Falls (SARC-F)	0	0
	1–3	1
	4–6	2
	7–10	3
Eastern Cooperative Oncology Group Performance Status (ECOG PS)	0	0
	1–2	1
	3–4	2
Appetite loss	0–3	0
	4–6	1
	7–10	2
Abnormal biochemistry (WBC $>$ 10 $\times$ 10^9/L, Alb $<$ 35 g/L; Hb $<$ 120/110 g/L)	All normal	0
	One abnormal	1
	More than one abnormal	2

Weight loss last 6 mo

Select what applies:

Weight is stable or gained weight	0
Weight loss $\leq$ 5%	1
Weight loss $\geq$ 5% and $\leq$ 15%	2
Weight loss $\geq$ 15%	3

SARC-F questionnaire

Select what applies:

Strength: How difficult is it for you to lift and carry a 5 kg bag?

a. Easy = 0
b. A little difficult = 1
c. Very difficult or impossible = 2

Assistance with walking: How difficult is it for you to walk across a room?

a. Easy = 0
b. A little difficult = 1
c. Very difficult or impossible = 2

Getting up from a chair: How difficult is it for you to get up from a chair or bed?

a. Easy = 0
b. A little difficult = 1
c. Very difficult or impossible = 2

Climbing stairs: How difficult is it for you to climb ten steps?

a. Easy = 0
b. A little difficult = 1
c. Very difficult or impossible = 2

Falling: How many times have you fallen in the past year?

a. None = 0
b. 1–3 times = 1
c. 4 times or more = 2

Total score

0	0
1–3	1
4–6	2
7–10	3

ECOG-PS

Select what applies:

0 = Fully active, able to carry on all predisease activities without restriction

1 = Restricted in physically strenuous activity but ambulatory and able to carry out light or sedentary work, e.g., light housework, office work

2 = Ambulatory and capable of all self-care but unable to carry out any work activities; up and about more than 50% of waking hours

3 = Capable of only limited self-care; confined to bed or chair more than 50% of waking hours

4 = Completely disabled; cannot carry on any self-care; totally confined to bed or chair

0	0
1–2	1
3–4	2

Reduced appetite

Indicate what applies:

Score from 0–10

0 = no reduced appetite

10 = no appetite at all

0–3	0
4–6	1
7–10	2

Abnormal biochemistry

Indicate what applies:

- White blood cells $> 10 \times 10^9$/L
- Albumin < 35 g/L
- Hemoglobin $< 120/110$ g/L

All normal	0
One of the three abnormal	1
More than one abnormal	2

Total score of the 5 categories

- 0–2: noncachexia
- 3–4: precachexia
- 5–8: cachexia
- 9–12: refractory cachexia

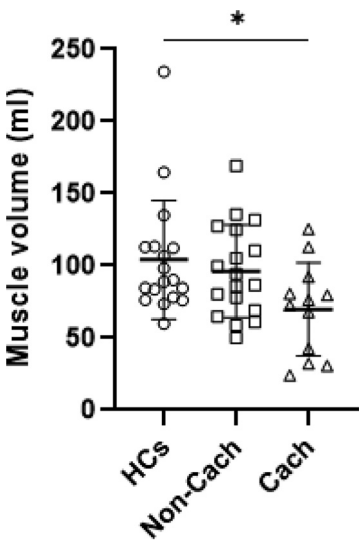

Figure A1. Muscle volume of the *m. rectus femoris*. Healthy controls (HCs) are represented as ○ ($n = 18$), patients with colorectal cancer (CRC) without cachexia as □ ($n = 18$), and patients with CRC-associated cachexia as △ ($n = 12$). Data are presented as individual values and means ± SD. *$P <$ 0.05. cach, cachectic; noncach, noncachectic; SD, standard deviation.

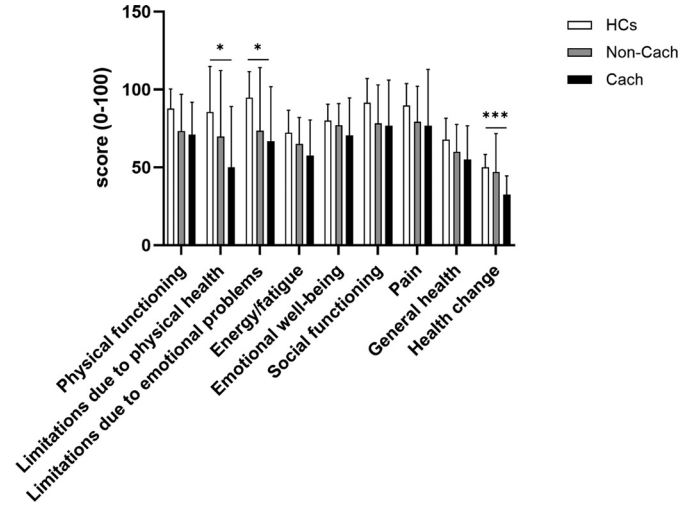

Figure A2. Scores (0–100) across different domains of the 36-item Short Form Survey (SF-36). Healthy controls (HCs) ($n = 19$) are presented as the white bars, patients with colorectal cancer (CRC) without cachexia ($n = 24$) as gray bars, and patients with CRC-associated cachexia ($n = 10$) as black bars. Data are presented as means ± SD. *$P < 0.05$, ***$P < 0.001$. cach, cachectic; noncach, noncachectic.

Table A2. *Primary and secondary antibodies for immunohistochemistry*

Target	Goal	Primary Antibody	Dilution	Firm
Laminin	Fiber border	Polyclonal Rabbit anti-laminin IgG (Ab11575)	1/50	Developmental Studies Hybridoma Bank, Iowa City, Iowa, USA
MHC-1	Fiber type I	Monoclonal Mouse anti-MHC IgG2b (BA-F8-s)	1/50	Abcam, Cambridge, UK
CD31	Capillarization	Monoclonal Mouse anti-human CD31 IgG1 (M0823)	1/50	Agilent Technologies, Santa Clara, California, USA
Goal		**Secondary antibodies**	**Dilution**	**Firm**
Fiber border		Polyclonal Goat anti-rabbit IgG AF647 (A21245)	1/400	Thermo Fisher Scientific, Waltham, Massachusetts, USA
Fiber type I		Polyclonal Goat anti-mouse IgG2b AF488 (A21141)	1/400	Thermo Fisher Scientific, Waltham, Massachusetts, USA
Capillarization		Horse anti-mouse IgG (BA-2000) Texas Red Avidin D (A-2006)	1/200 1/400	Vector Laboratories, Newark, California, USA

AF, Alexa Fluor; MHC, myosin heavy chain.

Table A3. *Post hoc power calculations for the different outcome measures*

Outcome Measure	Effect Size	Power
m. vastus lateralis		
CSA, μm^2		
Type I fibers	0.21	0.13
Type II fibers	1.39	0.98
Fiber type distribution, %		
Type I fibers	0.66	0.53
Type II fibers	0.66	0.53
RCSA, %		
Type I fibers	0.13	0.10
Type II fibers	0.13	0.10
Number myonuclei/fiber		
Type I fibers	1.04	0.86
Type II fibers	2.00	0.99
Myonuclear domain, μm^2		
Type I fibers	1.15	0.91
Type II fibers	0.58	0.45
Number central nuclei/fiber		
Type I fibers	0.61	0.49
Type II fibers	0.21	0.14
C:F	0.75	0.63
CFD		
Type I fibers	0.66	0.53
Type II fibers	0.05	0.07
m. erector spinae		
CSA, μm^2		
Type I fibers	0.77	0.63
Type II fibers	0.30	0.19
Fiber type distribution (%)		
Type I fibers	0.76	0.62
Type II fibers	0.76	0.62
RCSA, %		
Type I fibers	0.70	0.57
Type II fibers	0.70	0.57
Number myonuclei/fiber		
Type I fibers	1.07	0.87
Type II fibers	0.99	0.82
Myonuclear domain, μm^2		
Type I fibers	0.26	0.16
Type II fibers	0.90	0.75
Number central nuclei/fiber		
Type I fibers	0.66	0.53
Type II fibers	0.50	0.37
C:F	0.58	0.44
CFD		
Type I fibers	0.01	0.05
Type II fibers	0.25	0.16
CT-scan CSA, mm^2, m. erector spinae	0.73	0.63
CT-scan CSA, mm^2/patient body height^2, m^2, m. erector spinae	0.64	0.53
CT-scan HU, m. erector spinae	0.89	0.78
SPPB total score	1.37	0.97
Walk speed	0.86	0.73
Sit-to-stand	1.37	0.97
Balance	0.51	0.38
Handgrip strength, kg	1.11	0.91
PASIPD	0.27	0.19
SF-36	1.29	0.94

C:F, capillary to fiber ratio; CFD, capillary fiber density; CSA, cross-sectional area; CT, computed tomography; HU, Hounsfield Units; m., muscle; PASIPD, Physical Activity Scale for Individuals with Physical Disabilities; RCSA, relative cross-sectional area; SF-36, 36-item Short Form Survey; SPPB, Short Physical Performance Battery.

Table A4. *Tumor location and staging*

	Tumor Location	TNM Staging	Metastasis
Patients with colorectal cancer-associated cachexia			
CCP1	Sigmoid	T3N0M1	Yes
CCP2	Ascending colon	T3N2M0	No
CCP3	Rectum	T3N2M0	No
CCP4	Ascending colon	T4N1M0	No
CCP5	Cecum	T3N0M0	No
CCP6	Hepatic flexure	T3N0M0	No
CCP7	Cecum	T4N1M0	No
CCP8	Descending colon	T3N2M0	No
CCP9	Cecum	T1N0M0	No
CCP10	Transverse colon	T4N1M0	No
CCP11	Sigmoid	T3N1M0	No
CCP12	Ascending colon	T3N0M0	No
Patients with colorectal cancer without cachexia			
CCP13	Sigmoid	T3N1M0	No
CCP14	Distal rectum	T3N2M0	No
CCP15	Sigmoid	T2N1M0	No
CCP16	Descending colon	T3N0M0	No
CCP17	Ileum	T2N1M0	No
CCP18	Distal rectum	T3N1M0	No
CCP19	Cecum	T2N0M0	No
CCP20	Sigmoid	T3N0M0	No
CCP21	Mid rectum	T3N1M0	No
CCP22	Distal rectum	T3N0M0	No
CCP23	Distal rectum	T3N0M0	No
CCP24	Distal rectum	T3N1M0	No
CCP25	Cecum	T3N0M0	No
CCP26	Hepatic flexure	TisN0M0	No
CCP27	Ileum	T4N1M0	No
CCP28	Rectosigmoid	T2N0M0	No
CCP29	Sigmoid	/	/
CCP30	Ascending colon	T1N0M0	No
CCP31	Distal rectum	T1N0M0	No
CCP32	Proximal rectum	T3N1M0	No
CCP33	Cecum	T3N0M0	No
CCP34	Sigmoid	T4N0M0	No
CCP35	Sigmoid	T1N0M0	No
CCP36	Sigmoid	T2N0M0	No
CCP37	Proximal rectum	T1N0M0	No

DATA AVAILABILITY

Data will be made available upon reasonable request.

ACKNOWLEDGMENTS

We thank all patients and healthy controls for participation in the study. Furthermore, we want to thank abdominal surgeons Dr. B. Houben, Dr. K. Vandesteen, and Dr. R. Blom for their support with recruitment and biopsy collection during the study. Graphical abstract made with a licensed version of BioRender.com.

GRANTS

This study was funded by Limburgs Kankerfonds (LIKAF) (to Anouk Agten and Frank Vandenabeele).

DISCLOSURES

No conflicts of interest, financial or otherwise, are declared by the authors.

AUTHOR CONTRIBUTIONS

B.v.d.H., B.H., F.V., K.V., and A.A. conceived and designed research; B.v.d.H. and M.H. performed experiments; B.v.d.H. and M.H. analyzed data; B.v.d.H., M.E.G.W., K.V., and A.A. interpreted results of experiments; B.v.d.H. prepared figures; B.v.d.H. drafted manuscript; B.v.d.H., M.H., B.H., M.E.G.W., F.V., K.V., and A.A. edited and revised manuscript; B.v.d.H., M.H., B.H., M.E.G.W., F.V., K.V., and A.A. approved final version of manuscript.

REFERENCES

1. **Argilés JM**, **Busquets S**, **Stemmler B**, **López-Soriano FJ.** Cachexia and sarcopenia: mechanisms and potential targets for intervention. *Curr Opin Pharmacol* 22: 100–106, 2015. doi:10.1016/j.coph.2015.04.003.
2. **Pin F**, **Couch ME**, **Bonetto A.** Preservation of muscle mass as a strategy to reduce the toxic effects of cancer chemotherapy on body composition. *Curr Opin Support Palliat Care* 12: 420–426, 2018. doi:10.1097/SPC.0000000000000382.
3. **Renfro LA**, **Loupakis F**, **Adams RA**, **Seymour MT**, **Heinemann V**, **Schmoll H-J**, **Douillard J-Y**, **Hurwitz H**, **Fuchs CS**, **Diaz-Rubio E**, **Porschen R**, **Tournigand C**, **Chibaudel B**, **Falcone A**, **Tebbutt NC**, **Punt CJA**, **Hecht JR**, **Bokemeyer C**, **Van Cutsem E**, **Goldberg RM**, **Saltz LB**, **de Gramont A**, **Sargent DJ**, **Lenz HJ.** Body mass index is prognostic in metastatic colorectal cancer: pooled analysis of patients from first-line clinical trials in the ARCAD database. *J Clin Oncol* 34: 144–150, 2016. doi:10.1200/JCO.2015.61.6441.
4. **Sadeghi M**, **Keshavarz-Fathi M**, **Baracos V**, **Arends J**, **Mahmoudi M**, **Rezaei N.** Cancer cachexia: diagnosis, assessment, and treatment. *Crit Rev Oncol Hematol* 127: 91–104, 2018. doi:10.1016/j.critrevonc.2018.05.006.
5. **Malavaki CJ**, **Sakkas GK**, **Mitrou GI**, **Kalyva A**, **Stefanidis I**, **Myburgh KH**, **Karatzaferi C.** Skeletal muscle atrophy: disease-induced mechanisms may mask disuse atrophy. *J Muscle Res Cell Motil* 36: 405–421, 2015. doi:10.1007/s10974-015-9439-8.
6. **Mravec B.** Neurobiology of cancer: definition, historical overview, and clinical implications. *Cancer Med* 11: 903–921, 2022. doi:10.1002/cam4.4488.
7. **Wang YF**, **An ZY**, **Lin DH**, **Jin WL.** Targeting cancer cachexia: molecular mechanisms and clinical study. *MedComm (2020)* 3: e164, 2022. doi:10.1002/mco2.164.
8. **Han J**, **Harrison L**, **Patzelt L**, **Wu M**, **Junker D**, **Herzig S**, **Berriel Diaz M**, **Karampinos DC.** Imaging modalities for diagnosis and monitoring of cancer cachexia. *EJNMMI Res* 11: 94, 2021. doi:10.1186/s13550-021-00834-2.
9. **Mariean CR**, **Tiucă OM**, **Mariean A**, **Cotoi OS.** Cancer cachexia: new insights and future directions. *Cancers (Basel)* 15: 5590, 2023. doi:10.3390/cancers15235590.
10. **Kurk SA**, **Peeters PHM**, **Dorresteijn B**, **de Jong PA**, **Jourdan M**, **Kuijf HJ**, **Punt CJA**, **Koopman M**, **May AM.** Impact of different palliative systemic treatments on skeletal muscle mass in metastatic colorectal cancer patients. *J Cachexia Sarcopenia Muscle* 9: 909–919, 2018. doi:10.1002/jcsm.12337.
11. **Fearon K**, **Strasser F**, **Anker SD**, **Bosaeus I**, **Bruera E**, **Fainsinger RL**, **Jatoi A**, **Loprinzi C**, **MacDonald N**, **Mantovani G**, **Davis M**, **Muscaritoli M**, **Ottery F**, **Radbruch L**, **Ravasco P**, **Walsh D**, **Wilcock A**, **Kaasa S**, **Baracos VE.** Definition and classification of cancer cachexia: an international consensus. *Lancet Oncol* 12: 489–495, 2011. doi:10.1016/S1470-2045(10)70218-7.
12. **Ni J**, **Zhang L.** Cancer cachexia: definition, staging, and emerging treatments. *Cancer Manag Res* 12: 5597–5605, 2020. doi:10.2147/CMAR.S261585.
13. **Schiaffino S**, **Reggiani C.** Molecular diversity of myofibrillar proteins: gene regulation and functional significance. *Physiol Rev* 76: 371–423, 1996. doi:10.1152/physrev.1996.76.2.371.
14. **Caiozzo VJ.** Plasticity of skeletal muscle phenotype: mechanical consequences. *Muscle Nerve* 26: 740–768, 2002. doi:10.1002/mus.10271.
15. **Scott W**, **Stevens J**, **Binder-Macleod SA.** Human skeletal muscle fiber type classifications. *Phys Ther* 81: 1810–1816, 2001. doi:10.1093/ptj/81.11.1810.
16. **Chacon-Cabrera A**, **Fermoselle C**, **Urtreger AJ**, **Mateu-Jimenez M**, **Diament MJ**, **de Kier Joffé ED**, **Sandri M**, **Barreiro E.** Pharmacological strategies in lung cancer-induced cachexia: effects on muscle proteolysis, autophagy, structure, and weakness. *J Cell Physiol* 229: 1660–1672, 2014. doi:10.1002/jcp.24611.
17. **Salazar-Degracia A**, **Blanco D**, **Vilà-Ubach M**, **de Biurrun G**, **de Solórzano CO**, **Montuenga LM**, **Barreiro E.** Phenotypic and metabolic features of mouse diaphragm and gastrocnemius muscles in chronic lung carcinogenesis: influence of underlying emphysema. *J Transl Med* 14: 244, 2016. doi:10.1186/s12967-016-1003-9.
18. **Bohnert KR**, **Gallot YS**, **Sato S**, **Xiong G**, **Hindi SM**, **Kumar A.** Inhibition of ER stress and unfolding protein response pathways causes skeletal muscle wasting during cancer cachexia. *FASEB J* 30: 3053–3068, 2016. doi:10.1096/fj.201600250RR.
19. **Schwarzkopf M**, **Coletti D**, **Sassoon D**, **Marazzi G.** Muscle cachexia is regulated by a p53-PW1/Peg3-dependent pathway. *Genes Dev* 20: 3440–3452, 2006. doi:10.1101/gad.412606.
20. **Op den Kamp CM**, **Gosker HR**, **Lagarde S**, **Tan DY**, **Snepvangers FJ**, **Dingemans AM**, **Langen RCJ**, **Schols AM.** Preserved muscle oxidative metabolic phenotype in newly diagnosed non-small cell lung cancer cachexia. *J Cachexia Sarcopenia Muscle* 6: 164–173, 2015. doi:10.1002/jcsm.12007.
21. **Johns N**, **Hatakeyama S**, **Stephens NA**, **Degen M**, **Degen S**, **Frieauff W**, **Lambert C**, **Ross JA**, **Roubenoff R**, **Glass DJ**, **Jacobi C**, **Fearon KC.** Clinical classification of cancer cachexia: phenotypic correlates in human skeletal muscle. *PLoS One* 9: e83618, 2014 [Erratum in *PLoS One* 19: e0314953, 2024]. doi:10.1371/journal.pone.0083618.
22. **Julienne CM**, **Dumas JF**, **Goupille C**, **Pinault M**, **Berri C**, **Collin A**, **Tesseraud S**, **Couet C**, **Servais S.** Cancer cachexia is associated with a decrease in skeletal muscle mitochondrial oxidative capacities without alteration of ATP production efficiency. *J Cachexia Sarcopenia Muscle* 3: 265–275, 2012. doi:10.1007/s13539-012-0071-9.
23. **Shum AM**, **Mahendradatta T**, **Taylor RJ**, **Painter AB**, **Moore MM**, **Tsoli M**, **Tan TC**, **Clarke SJ**, **Robertson GR**, **Polly P.** Disruption of MEF2C signaling and loss of sarcomeric and mitochondrial integrity in cancer-induced skeletal muscle wasting. *Aging (Albany NY)* 4: 133–143, 2012. doi:10.18632/aging.100436.
24. **Acharyya S**, **Butchbach ME**, **Sahenk Z**, **Wang H**, **Saji M**, **Carathers M**, **Ringel MD**, **Skipworth RJ**, **Fearon KC**, **Hollingsworth MA**, **Muscarella P**, **Burghes AH**, **Rafael-Fortney JA**, **Guttridge DC.** Dystrophin glycoprotein complex dysfunction: a regulatory link between muscular dystrophy and cancer cachexia. *Cancer Cell* 8: 421–432, 2005. doi:10.1016/j.ccr.2005.10.004.
25. **Puig-Vilanova E**, **Rodriguez DA**, **Lloreta J**, **Ausin P**, **Pascual-Guardia S**, **Broquetas J**, **Roca J**, **Gea J**, **Barreiro E.** Oxidative stress, redox signaling pathways, and autophagy in cachectic muscles of male patients with advanced COPD and lung cancer. *Free Radic Biol Med* 79: 91–108, 2015. doi:10.1016/j.freeradbiomed.2014.11.006.
26. **Weber MA**, **Kinscherf R**, **Krakowski-Roosen H**, **Aulmann M**, **Renk H**, **Künkele A**, **Edler L**, **Kauczor HU**, **Hildebrandt W.** Myoglobin plasma level related to muscle mass and fiber composition: a clinical marker of muscle wasting? *J Mol Med (Berl)* 85: 887–896, 2007. doi:10.1007/s00109-007-0220-3.
27. **Taskin S**, **Stumpf VI**, **Bachmann J**, **Weber C**, **Martignoni ME**, **Friedrich O.** Motor protein function in skeletal abdominal muscle of cachectic cancer patients. *J Cell Mol Med* 18: 69–79, 2014. doi:10.1111/jcmm.12165.
28. **Schmitt TL**, **Martignoni ME**, **Bachmann J**, **Fechtner K**, **Friess H**, **Kinscherf R**, **Hildebrandt W.** Activity of the Akt-dependent anabolic and catabolic pathways in muscle and liver samples in cancer-related cachexia. *J Mol Med (Berl)* 85: 647–654, 2007 [Erratum in *J Mol Med* 85: 655–656, 2007]. doi:10.1007/s00109-007-0177-2.
29. **Brooks NE**, **Myburgh KH.** Skeletal muscle wasting with disuse atrophy is multi-dimensional: the response and interaction of myonuclei, satellite cells and signaling pathways. *Front Physiol* 5: 99, 2014. doi:10.3389/fphys.2014.00099.
30. **Daou N**, **Hassani M**, **Matos E**, **De Castro GS**, **Costa RGF**, **Seelaender M**, **Moresi V**, **Rocchi M**, **Adamo S**, **Li Z**, **Agbulut O**, **Coletti D.** Displaced myonuclei in cancer cachexia suggest altered innervation. *Int J Mol Sci* 21: 1092, 2020. doi:10.3390/ijms21031092.

31. **Hendrickse P**, **Degens H.** The role of the microcirculation in muscle function and plasticity. *J Muscle Res Cell Motil* 40: 127–140, 2019. doi:10.1007/s10974-019-09520-2.
32. **Tanaka M**, **Sugimoto K**, **Fujimoto T**, **Xie K**, **Takahashi T**, **Akasaka H**, **Yasunobe Y**, **Takeya Y**, **Yamamoto K**, **Hirabayashi T**, **Fujino H**, **Rakugi H.** Differential effects of pre-exercise on cancer cachexia-induced muscle atrophy in fast- and slow-twitch muscles. *FASEB J* 34: 14389–14406, 2020. doi:10.1096/fj.202001330R.
33. **Tanaka M**, **Sugimoto K**, **Fujimoto T**, **Xie K**, **Takahashi T**, **Akasaka H**, **Kurinami H**, **Yasunobe Y**, **Matsumoto T**, **Fujino H**, **Rakugi H.** Preventive effects of low-intensity exercise on cancer cachexia-induced muscle atrophy. *FASEB J* 33: 7852–7862, 2019. doi:10.1096/fj.201802430R.
34. **Tang K**, **Wagner PD**, **Breen EC.** TNF-α-mediated reduction in PGC-1α may impair skeletal muscle function after cigarette smoke exposure. *J Cell Physiol* 222: 320–327, 2010. doi:10.1002/jcp.21955.
35. **Morena F**, **Cabrera AR**, **Greene NP.** Exploring heterogeneity: a dive into preclinical models of cancer cachexia. *Am J Physiol Cell Physiol* 327: C310–C328, 2024. doi:10.1152/ajpcell.00317.2024.
36. **Martin A**, **Freyssenet D.** Phenotypic features of cancer cachexia-related loss of skeletal muscle mass and function: lessons from human and animal studies. *J Cachexia Sarcopenia Muscle* 12: 252–273, 2021. doi:10.1002/jcsm.12678.
37. **Anderson LJ**, **Lee J**, **Mallen MC**, **Migula D**, **Liu H**, **Wu PC**, **Dash A**, **Garcia JM.** Evaluation of physical function and its association with body composition, quality of life and biomarkers in cancer cachexia patients. *Clin Nutr* 40: 978–986, 2021. doi:10.1016/j.clnu.2020.07.001.
38. **Dohzono S**, **Sasaoka R**, **Takamatsu K**, **Hoshino M**, **Nakamura H.** Prognostic value of paravertebral muscle density in patients with spinal metastases from gastrointestinal cancer. *Support Care Cancer* 27: 1207–1213, 2019. doi:10.1007/s00520-018-4465-x.
39. **Molwitz I**, **Leiderer M**, **McDonough R**, **Fischer R**, **Ozga AK**, **Ozden C**, **Tahir E**, **Koehler D**, **Adam G**, **Yamamura J.** Skeletal muscle fat quantification by dual-energy computed tomography in comparison with 3T MR imaging. *Eur Radiol* 31: 7529–7539, 2021. doi:10.1007/s00330-021-07820-1.
40. **Cruz-Jentoft AJ**, **Bahat G**, **Bauer J**, **Boirie Y**, **Bruyère O**, **Cederholm T**, **Cooper C**, **Landi F**, **Rolland Y**, **Sayer AA**, **Schneider SM**, **Sieber CC**, **Topinkova E**, **Vandewoude M**, **Visser M**, **Zamboni M**; **Writing Group for the European Working Group on Sarcopenia in Older People 2 (EWGSOP2), and the Extended Group for EWGSOP2.** Sarcopenia: revised European consensus on definition and diagnosis. *Age Ageing*. 48: 16–31, 2019 [Erratum in *Age Ageing* 48: 601, 2019]. doi:10.1093/ageing/afy169.
41. **Evans WJ**, **Morley JE**, **Argilés J**, **Bales C**, **Baracos V**, **Guttridge D**, **Jatoi A**, **Kalantar-Zadeh K**, **Lochs H**, **Mantovani G**, **Marks D**, **Mitch WE**, **Muscaritoli M**, **Najand A**, **Ponikowski P**, **Rossi Fanelli F**, **Schambelan M**, **Schols A**, **Schuster M**, **Thomas D**, **Wolfe R**, **Anker SD.** Cachexia: a new definition. *Clin Nutr* 27: 793–799, 2008. doi:10.1016/j.clnu.2008.06.013.
42. **Zhou T**, **Wang B**, **Liu H**, **Yang K**, **Thapa S**, **Zhang H**, **Li L**, **Yu S.** Development and validation of a clinically applicable score to classify cachexia stages in advanced cancer patients. *J Cachexia Sarcopenia Muscle* 9: 306–314, 2018. doi:10.1002/jcsm.12275.
43. **Agten A**, **Stevens S**, **Verbrugghe J**, **Timmermans A**, **Vandenabeele F.** Biopsy samples from the erector spinae of persons with nonspecific chronic low back pain display a decrease in glycolytic muscle fibers. *Spine J* 20: 199–206, 2020. doi:10.1016/j.spinee.2019.09.023.
44. **Lanferdini FJ**, **Viera HLS**, **Gidiel-Machado L**, **Leite-Nunes TD**, **Soldatelli IM**, **Porporatti LB**, **Matheus SC**, **Dos Santos DL**, **Saccol MF**, **Royes LFF.** Vastus lateralis muscle architecture, quality, and stiffness are determinants of maximal performance in athletes? *J Biomech* 180: 112491, 2025. doi:10.1016/j.jbiomech.2025.112491.
45. **Betz MW**, **Aussieker T**, **Kruger CQ**, **Gorissen SHM**, **van Loon LJC**, **Snijders T.** Muscle fiber capillarization is associated with various indices of skeletal muscle mass in healthy, older men. *Exp Gerontol* 143: 111161, 2021. doi:10.1016/j.exger.2020.111161.
46. **Rummens S**, **Dierckx S**, **Brumagne S**, **Desloovere K**, **Peers K.** Three-dimensional freehand ultrasonography to measure muscle volume of the lumbar multifidus: reliability of processing technique and validity through comparison to magnetic resonance imaging. *J Anat* 244: 601–609, 2024. doi:10.1111/joa.13988.
47. **Engelke K**, **Museyko O**, **Wang L**, **Laredo JD.** Quantitative analysis of skeletal muscle by computed tomography imaging—state of the art. *J Orthop Translat* 15: 91–103, 2018. doi:10.1016/j.jot.2018.10.004.
48. **Bradley NA**, **Walter A**, **Dolan R**, **Wilson A**, **Siddiqui T**, **Roxburgh CSD**, **McMillan DC**, **Guthrie GJK.** Evaluation of the prognostic value of computed tomography-derived body composition in patients undergoing endovascular aneurysm repair. *J Cachexia Sarcopenia Muscle* 14: 1836–1847, 2023. doi:10.1002/jcsm.13262.
49. **de Groot S**, **van der Woude LH**, **Niezen A**, **Smit CA**, **Post MW.** Evaluation of the physical activity scale for individuals with physical disabilities in people with spinal cord injury. *Spinal Cord* 48: 542–547, 2010. doi:10.1038/sc.2009.178.
50. **Zhang Y**, **Dos Santos M**, **Huang H**, **Chen K**, **Iyengar P**, **Infante R**, **Polanco PM**, **Brekken RA**, **Cai C**, **Caijgas A**, **Cano Hernandez K**, **Xu L**, **Bassel-Duby R**, **Liu N**, **Olson EN.** A molecular pathway for cancer cachexia-induced muscle atrophy revealed at single-nucleus resolution. *Cell Rep* 43: 114587, 2024. doi:10.1016/j.celrep.2024.114587.
51. **Delfinis LJ**, **Bellissimo CA**, **Gandhi S**, **DiBenedetto SN**, **Garibotti MC**, **Thuhan AK**, **Tsitkanou S**, **Rosa-Caldwell ME**, **Rahman FA**, **Cheng AJ**, **Wiggs MP**, **Schlattner U**, **Quadrilatero J**, **Greene NP**, **Perry CG.** Muscle weakness precedes atrophy during cancer cachexia and is linked to muscle-specific mitochondrial stress. *JCI Insight* 7: e155147, 2022. doi:10.1172/jci.insight.155147.
52. **Zhang Y**, **Wang J**, **Wang X**, **Gao T**, **Tian H**, **Zhou D**, **Zhang L**, **Li G**, **Wang X.** The autophagic-lysosomal and ubiquitin proteasome systems are simultaneously activated in the skeletal muscle of gastric cancer patients with cachexia. *Am J Clin Nutr* 111: 570–579, 2020. doi:10.1093/ajcn/nqz347.
53. **White JP**, **Baltgalvis KA**, **Puppa MJ**, **Sato S**, **Baynes JW**, **Carson JA.** Muscle oxidative capacity during IL-6-dependent cancer cachexia. *Am J Physiol Regul Integr Comp Physiol* 300: R201–R211, 2011. doi:10.1152/ajpregu.00300.2010.
54. **Diffee GM**, **Kalfas K**, **Al-Majid S**, **McCarthy DO.** Altered expression of skeletal muscle myosin isoforms in cancer cachexia. *Am J Physiol Cell Physiol* 283: C1376–C1382, 2002. doi:10.1152/ajpcell.00154.2002.
55. **Marin-Corral J**, **Fontes CC**, **Pascual-Guardia S**, **Sanchez F**, **Olivan M**, **Argilés JM**, **Busquets S**, **López-Soriano FJ**, **Barreiro E.** Redox balance and carbonylated proteins in limb and heart muscles of cachectic rats. *Antioxid Redox Signal* 12: 365–380, 2010. doi:10.1089/ars.2009.2818.
56. **Murphy KT**, **Struk A**, **Malcontenti-Wilson C**, **Christophi C**, **Lynch GS.** Physiological characterization of a mouse model of cachexia in colorectal liver metastases. *Am J Physiol Regul Integr Comp Physiol* 304: R854–R864, 2013. doi:10.1152/ajpregu.00057.2013.
57. **Sun R**, **Zhang S**, **Lu X**, **Hu W**, **Lou N**, **Zhao Y**, **Zhou J**, **Zhang X**, **Yang H.** Comparative molecular analysis of early and late cancer cachexia-induced muscle wasting in mouse models. *Oncol Rep* 36: 3291–3302, 2016. doi:10.3892/or.2016.5165.
58. **Shenkman BS**, **Turtikova OV**, **Nemirovskaya TL**, **Grigoriev AI.** Skeletal muscle activity and the fate of myonuclei. *Acta Naturae* 2: 59–66, 2010. doi:10.32607/20758251-2010-2-2-59-65.
59. **Judge SM**, **Nosacka RL**, **Delitto D**, **Gerber MH**, **Cameron ME**, **Trevino JG**, **Judge AR.** Skeletal muscle fibrosis in pancreatic cancer patients with respect to survival. *JNCI Cancer Spectr* 2: pky043, 2018. doi:10.1093/jncics/pky043.
60. **Zampieri S**, **Doria A**, **Adami N**, **Biral D**, **Vecchiato M**, **Savastano S**, **Corbianco S**, **Carraro U**, **Merigliano S.** Subclinical myopathy in patients affected with newly diagnosed colorectal cancer at clinical onset of disease: evidence from skeletal muscle biopsies. *Neurol Res* 32: 20–25, 2010. doi:10.1179/016164110X12556180205997.
61. **Salazar-Degracia A**, **Busquets S**, **Argilés JM**, **Bargalló-Gispert N**, **López-Soriano FJ**, **Barreiro E.** Effects of the beta$_2$ agonist formoterol on atrophy signaling, autophagy, and muscle phenotype in respiratory and limb muscles of rats with cancer-induced cachexia. *Biochimie* 149: 79–91, 2018. doi:10.1016/j.biochi.2018.04.009.
62. **He WA**, **Berardi E**, **Cardillo VM**, **Acharyya S**, **Aulino P**, **Thomas-Ahner J**, **Wang J**, **Bloomston M**, **Muscarella P**, **Nau P**, **Shah N**, **Butchbach MER**, **Ladner K**, **Adamo S**, **Rudnicki MA**, **Keller C**, **Coletti D**, **Montanaro F**, **Guttridge DC.** NF-κB-mediated Pax7 dysregulation in the muscle microenvironment promotes cancer cachexia. *J Clin Invest* 123: 4821–4835, 2013. doi:10.1172/JCI68523.
63. **Snijders T**, **Nederveen JP**, **Joanisse S**, **Leenders M**, **Verdijk LB**, **van Loon LJ**, **Parise G.** Muscle fibre capillarization is a critical factor in

muscle fibre hypertrophy during resistance exercise training in older men. *J Cachexia Sarcopenia Muscle* 8: 267–276, 2017. doi:10.1002/jcsm.12137.

64. **Mijwel S**, **Cardinale DA**, **Norrbom J**, **Chapman M**, **Ivarsson N**, **Wengström Y**, **Sundberg CJ**, **Rundqvist H.** Exercise training during chemotherapy preserves skeletal muscle fiber area, capillarization, and mitochondrial content in patients with breast cancer. *FASEB J* 32: 5495–5505, 2018. doi:10.1096/fj.201700968R.
65. **Weber MA**, **Krakowski-Roosen H**, **Schröder L**, **Kinscherf R**, **Krix M**, **Kopp-Schneider A**, **Essig M**, **Bachert P**, **Kauczor HU**, **Hildebrandt W.** Morphology, metabolism, microcirculation, and strength of skeletal muscles in cancer-related cachexia. *Acta Oncol* 48: 116–124, 2009. doi:10.1080/02841860802130001.
66. **Talbot J**, **Maves L.** Skeletal muscle fiber type: using insights from muscle developmental biology to dissect targets for susceptibility and resistance to muscle disease. *Wiley Interdiscip Rev Dev Biol* 5: 518–534, 2016. doi:10.1002/wdev.230.
67. **Moreno-Justicia R**, **Van der Stede T**, **Stocks B**, **Laitila J**, **Seaborne RA**, **Van de Loock A**, **Lievens E**, **Samodova D**, **Marín-Arraiza L**, **Dmytriyeva O**, **Browaeys R**, **Van Vossel K**, **Moesgaard L**, **Yigit N**, **Anckaert J**, **Weyns A**, **Van Thienen R**, **Sahl RE**, **Zanoteli E**, **Lawlor MW**, **Wierer M**, **Mestdagh P**, **Vandesompele J**, **Ochala J**, **Hostrup M**, **Derave W**, **Deshmukh AS.** Human skeletal muscle fiber heterogeneity beyond myosin heavy chains. *Nat Commun* 16: 1764, 2025. doi:10.1038/s41467-025-56896-6.
68. **Gray C**, **MacGillivray TJ**, **Eeley C**, **Stephens NA**, **Beggs I**, **Fearon KC**, **Greig CA.** Magnetic resonance imaging with k-means clustering objectively measures whole muscle volume compartments in sarcopenia/cancer cachexia. *Clin Nutr* 30: 106–111, 2011. doi:10.1016/j.clnu.2010.07.012.
69. **Stephens NA**, **Gray C**, **MacDonald AJ**, **Tan BH**, **Gallagher IJ**, **Skipworth RJ**, **Ross JA**, **Fearon KC**, **Greig CA.** Sexual dimorphism modulates the impact of cancer cachexia on lower limb muscle mass and function. *Clin Nutr* 31: 499–505, 2012. doi:10.1016/j.clnu.2011.12.008.
70. **Loumaye A**, **de Barsy M**, **Nachit M**, **Lause P**, **Frateur L**, **van Maanen A**, **Trefois P**, **Gruson D**, **Thissen JP.** Role of Activin A and myostatin in human cancer cachexia. *J Clin Endocrinol Metab* 100: 2030–2038, 2015. doi:10.1210/jc.2014-4318.
71. **Edge SB**, **Compton CC.** The American Joint Committee on Cancer: the 7th edition of the AJCC cancer staging manual and the future of TNM. *Ann Surg Oncol* 17: 1471–1474, 2010. doi:10.1245/s10434-010-0985-4.
72. **Mortellaro S**, **Triggiani S**, **Mascaretti F**, **Galloni M**, **Garrone O**, **Carrafiello G**, **Ghidini M.** Quantitative and qualitative radiological assessment of sarcopenia and cachexia in cancer patients: a systematic review. *J Pers Med* 14: 243, 2024. doi:10.3390/jpm14030243.
73. **Blackwell JEM**, **Herrod PJJ**, **Doleman B**, **Boyd-Carson H**, **Dolan D**, **Wheldon L**, **Brown SR**, **Banerjea A**, **Moug S**, **Lund JN**; **POMPOMM Collaborative.** CT-derived measures of muscle quantity and quality predict poorer outcomes from elective colorectal surgery: a UK multicentre retrospective cohort study. *Tech Coloproctol* 27: 1091–1098, 2023. doi:10.1007/s10151-023-02769-3.
74. **Vigneron C**, **Laousy O**, **Chassagnon G**, **Vakalopoulou M**, **Charpentier J**, **Alexandre J**, **Jamme M**, **Pène F.** Assessment of functional and nutritional status and skeletal muscle mass for the prognosis of critically ill solid cancer patients. *Cancers (Basel)* 14: 5870, 2022. doi:10.3390/cancers14235870.
75. **Hadzibegovic S**, **Porthun J**, **Lena A**, **Weinländer P**, **Lück LC**, **Potthoff SK**, **Rösnick L**, **Fröhlich AK**, **Ramer LV**, **Sonntag F**, **Wilkenshoff U**, **Ahn J**, **Keller U**, **Bullinger L**, **Mahabadi AA**, **Totzeck M**, **Rassaf T**, **von Haehling S**, **Coats AJS**, **Anker SD**, **Roeland EJ**, **Landmesser U**, **Anker MS.** Hand grip strength in patients with advanced cancer: a prospective study. *J Cachexia Sarcopenia Muscle* 14: 1682–1694, 2023. doi:10.1002/jcsm.13248.
76. **Ohmae N**, **Yasui-Yamada S**, **Furumoto T**, **Wada K**, **Hayashi H**, **Kitao M**, **Yamanaka A**, **Kubo M**, **Matsuoka M**, **Kamimura S**, **Shimada A**, **Sato N**, **Kitamura Y**, **Katoh S**, **Takeda N**, **Hamada Y.** Muscle mass, quality, and strength; physical function and activity; and metabolic status in cachectic patients with head and neck cancer. *Clin Nutr ESPEN* 53: 113–119, 2023. doi:10.1016/j.clnesp.2022.12.006.
77. **Dalise S**, **Tropea P**, **Galli L**, **Sbrana A**, **Chisari C.** Muscle function impairment in cancer patients in pre-cachexia stage. *Eur J Transl Myol* 30: 8931, 2020. doi:10.4081/ejtm.2020.8931.
78. **Shorter E**, **Engman V**, **Lanner JT.** Cancer-associated muscle weakness—from triggers to molecular mechanisms. *Mol Aspects Med* 97: 101260, 2024. doi:10.1016/j.mam.2024.101260.
79. **McPhee JS**, **Cameron J**, **Maden-Wilkinson T**, **Piasecki M**, **Yap MH**, **Jones DA**, **Degens H.** The contributions of fiber atrophy, fiber loss, in situ specific force, and voluntary activation to weakness in sarcopenia. *J Gerontol A Biol Sci Med Sci* 73: 1287–1294, 2018. doi:10.1093/gerona/gly040.
80. **Cole CL**, **Kleckner IR**, **Jatoi A**, **Schwarz EM**, **Dunne RF.** The role of systemic inflammation in cancer-associated muscle wasting and rationale for exercise as a therapeutic intervention. *JCSM Clin Rep* 3: e00065, 2018. doi:10.17987/jcsm-cr.v3i2.65.
81. **Fearon KC**, **Voss AC**, **Hustead DS**; **Cancer Cachexia Study Group.** Definition of cancer cachexia: effect of weight loss, reduced food intake, and systemic inflammation on functional status and prognosis. *Am J Clin Nutr* 83: 1345–1350, 2006. doi:10.1093/ajcn/83.6.1345.
82. **Bachmann J**, **Heiligensetzer M**, **Krakowski-Roosen H**, **Buchler MW**, **Friess H**, **Martignoni ME.** Cachexia worsens prognosis in patients with resectable pancreatic cancer. *J Gastrointest Surg* 12: 1193–1201, 2008. doi:10.1007/s11605-008-0505-z.
83. **Ravasco P**, **Monteiro-Grillo I**, **Vidal PM**, **Camilo ME.** Cancer: disease and nutrition are key determinants of patients' quality of life. *Support Care Cancer* 12: 246–252, 2004. doi:10.1007/s00520-003-0568-z.
84. **Fouladiun M**, **Körner U**, **Gunnebo L**, **Sixt-Ammilon P**, **Bosaeus I**, **Lundholm K.** Daily physical-rest activities in relation to nutritional state, metabolism, and quality of life in cancer patients with progressive cachexia. *Clin Cancer Res* 13: 6379–6385, 2007. doi:10.1158/1078-0432.CCR-07-1147.
85. **Mormont MC**, **Waterhouse J.** Contribution of the rest-activity circadian rhythm to quality of life in cancer patients. *Chronobiol Int* 19: 313–323, 2002. doi:10.1081/cbi-120002606.
86. **Moses AW**, **Slater C**, **Preston T**, **Barber MD**, **Fearon KC.** Reduced total energy expenditure and physical activity in cachectic patients with pancreatic cancer can be modulated by an energy and protein dense oral supplement enriched with *n*-3 fatty acids. *Br J Cancer* 90: 996–1002, 2004. doi:10.1038/sj.bjc.6601620.
87. **Callahan DM**, **Bedrin NG**, **Subramanian M**, **Berking J**, **Ades PA**, **Toth MJ**, **Miller MS.** Age-related structural alterations in human skeletal muscle fibers and mitochondria are sex specific: relationship to single-fiber function. *J Appl Physiol (1985)* 116: 1582–1592, 2014. doi:10.1152/japplphysiol.01362.2013.
88. **Lauretani F**, **Russo CR**, **Bandinelli S**, **Bartali B**, **Cavazzini C**, **Di Iorio A**, **Corsi AM**, **Rantanen T**, **Guralnik JM**, **Ferrucci L.** Age-associated changes in skeletal muscles and their effect on mobility: an operational diagnosis of sarcopenia. *J Appl Physiol (1985)* 95: 1851–1860, 2003. doi:10.1152/japplphysiol.00246.2003.
89. **Staron RS**, **Hagerman FC**, **Hikida RS**, **Murray TF**, **Hostler DP**, **Crill MT**, **Ragg KE**, **Toma K.** Fiber type composition of the vastus lateralis muscle of young men and women. *J Histochem Cytochem* 48: 623–629, 2000. doi:10.1177/002215540004800506.
90. **Haizlip KM**, **Harrison BC**, **Leinwand LA.** Sex-based differences in skeletal muscle kinetics and fiber-type composition. *Physiology (Bethesda)* 30: 30–39, 2015. doi:10.1152/physiol.00024.2014.